

ON THE MECHANISM OF SOLID SURFACE AND TEMPERATURE
PROGRAMMED DESORPTION AND ITS APPLICATION AS A DETECTION TECHNIQUE
FOR HIGH PERFORMANCE LIQUID CHROMATOGRAPHY

BY

JAMES DONALD CARTER

A DISSERTATION PRESENTED TO THE GRADUATE SCHOOL
OF THE UNIVERSITY OF FLORIDA IN PARTIAL FULFILLMENT
OF THE REQUIREMENTS FOR THE DEGREE OF
DOCTOR OF PHILOSOPHY

UNIVERSITY OF FLORIDA LIBRARY

UNIVERSITY OF FLORIDA

1980
FOL 1

ACKNOWLEDGMENTS

I would like to express my gratitude to the Conselho Nacional de Desenvolvimento Científico e Tecnológico — CNPQ for the last year fellowship that has made possible my studies at the University of Florida, and to the Universidade de Brasília for permission to leave.

I am very grateful to Dr. James E. Winfree for the opportunity of joining his research group, and for his patience and his concern throughout my stay in Gainesville, FL.

I also express my gratitude to those that have made the difference in the achievement of my goals. To my family, which has always supported me with love and care. To Dr. Winston C. De Lima for his example as a professional and human being. To Luciana D. Blum for her support and love during my most difficult moments in Gainesville. And to Martin E. Mendonça for her love and care in the last part of my studies.

Finally, but not least, I would like to thank all the members of Dr. James E. Winfree's group for their friendship, especially Edith Torres, Jane Lammey, Jorge Vaz, Lynn Perry, Bruce Castellanos, and Josef Hinesmann, and Susan Clemons for the excellent job in typing this dissertation.

TABLE OF CONTENTS

	Page
ACKNOWLEDGMENTS	vi
LIST OF TABLES	v
LIST OF FIGURES	vi
ABSTRACT	xi
CHAPTERS	
1 INTRODUCTION TO FLOW-INJECTION	1
Solid State Process	1
Quantum Yield	8
Lifetime of Phosphors	1
The Heavy Atom Effect	8
Phosphorescence as an analytical Technique	8
2 EXPERIMENTAL CONSIDERATIONS FOR SOLID SURFACE	
HIGH THROUGHPUT FLOW-INJECTION	14
Scavenging Effects	18
Background Influence on IRRF	21
Internal Heavy Atom Effect	24
3 AUTOMATIC SAMPLING DESIGN FOR HETEROGENEOUS	38
Introduction	38
Instrumentation	42
Reagents	48
Procedures	48
Automatic System Employing an Atomic Absorption Detector	
Preparation of Toluene (D) Grouped Solvents	49
Preparation of Solutions	49
Measurement Procedure	49
Automatic System Employing Two Spectroscopic Detectors	49
Preparation of Solutions	49
Measurement Procedure	49
Results and Discussion	49
Conclusions	49
4 SOLID SURFACE HIGH THROUGHPUT FLOW-INJECTION	
DESIGN FOR HIGH PERFORMANCE LIQUID CHROMATOGRAPHY	58
Introduction	58
Flow Injection Analysis for Continuous Sample	
Introduction to HPLC	60
Equilibrium	60
Instrumentation	60
Reagents	60

	Procedure	52
	Results and Discussion	58
	Validation of a Flow Detector Assembly System as a Continuous HPLC Detector for HPLC analysis	61
	Experimental	61
	Instrumentation	61
	Reagents	61
	Procedure	64
	Results and Discussion	67
	Chromatographic Peak Broadening	67
	Flow Rate Effect	68
	Analytical Figures of Merit	67
	Symbol Figures	71
	Conclusions	78
5	HPLC SYSTEMS WITH TEMPERATURE PROGRAMMABLE DETECTION OF CATIONIC TERMOPLASTIC AND TERMOPLASTIC IN HIGH PRESSURE LIQUID CHROMATOGRAPHY	88
	Introduction	88
	Experimental	90
	Instrumentation	90
	Reagents	90
	Procedure	91
	Results and Discussion	94
	Flow Rate Effect	95
	Chromatographic Peak Broadening	94
	Analytical Figures of Merit	96
	HPLC Detection of Cationic, Thermoplastic and Thermoplastic in High Pressure	98
	Conclusions	100
6	CHROMATOGRAPHY AND SENSITIVITY FOR FLOW RATE	104
	INTRODUCTION	104
	EXPERIMENTAL SECTION	104

LIST OF TABLES

Table		Page
3-1	analytical Figures of Merit Obtained for Solid Substrate Room Temperature Fluorescentary With an Automatic Sampling System Employing an Atomic Absorption Substrate as Injection Introduction Device	44
3-2	analytical Figures of Merit Obtained for Solid Substrate Room Temperature Fluorescentary With an Automatic Sampling System Employing Two Substrates as Heavy atom and Analyte Introduction Devices	48
4-1	Analytic Determinations Employed With the Mixing Ratio System with a Flow Injection Analysis System as a Continuous Sampling Introduction Device for Solid Substrate Room Temperature Fluorescentary	53
4-2	Analytical Figures of Merit Obtained With Flow Injection Analysis System as a Continuous Sampling Introduction Device for Solid Substrate Room Temperature Fluorescentary Analysis	58
4-3	Wavelength Intensity Enlarged and Chromatographic Parameters Obtained by High Performance Liquid Chromatography With UV Absorption and Solid Substrate Room Temperature Fluorescentary Detection	63
4-4	analytical Figures of Merit Obtained for High Performance Liquid Chromatography Using Solid Substrate Room Temperature Fluorescentary and UV Absorption Detection	71

3.1.	Room Temperature Morphological Characteristics of Cellulose, Thapsyllins, and Thapsyrins on Filter Paper: Selected Scopy with Effect.	70
3.1.1.	Chromatographic Methods: Utilized by UV Absorption and IRFT Spectroscopy in the HPLC Analysis of Thapsyrins, Thapsyllins, and Cellulose	74
3.1.2.	Analytical Figures of Merit Derived for Thapsyrins, Thapsyllins, and Cellulose by High Performance Liquid Chromatography with In-Line Ultraviolet Room Temperature Morphology and UV Detection	100
3.2.	Effect of Storage Upon the Room Temperature Morphological Characteristics of Cellulose, Thapsyllins and Thapsyrins	118

LIST OF FIGURES

Figure

- 1-1 Schematic diagram showing the different radiation and conversion processes that can occur in a molecule upon excitation into a singlet state. S_0 , in absorption; S_1 , fluorescence; I , internal conversion; ISC , intersystem crossing; P_1 , phosphorescence; NR , nonradiative relaxation.
- 1-2 Schematic diagram of a Berlin Glass LB-1 Spectrofluorimeter.
 R_1 , mirror
 S , slit
 G , grating
 SL , beam splitter
 V_1 , viewport
REF REF, reference photomultiplier tube
SAMPLE REF, sample photomultiplier tube
PMT, phototube
- 1-3 Schematic diagram of a Filter paper guide used for a continuous solid substrate room temperature phosphorescence sampling system.
(a) Front view of the filter paper guide during the excitation source of the spectrofluorimeter. (b) Side view of the filter paper guide during the monochromator continuous filter.
(c) Front view of the filter paper guide.
- 1-4 Side view of an automatic sampling system for continuous solid substrate room temperature phosphorescence analysis employing an excitation source. (1) Filter paper roll. (2) excitation source. (3) Sample chamber. (4) Spectrofluorimeter. (5) Modified sample response. (6) monochromator continuous filter.
- 1-5 Side view of an automatic sampling system for continuous solid substrate room temperature phosphorescence analysis employing an excitation source. (1) Filter paper roll. (2) excitation source. (3) Sample chamber. (4) Sample response. (5) monochromator continuous filter.

substituted: (13) drying chamber; (14) heated sample compartment; (15) photomultiplier	
(16) multichannel continuous filter	68
4-1. Flow injection analysis system used as a continuous sample introduction device for automated solid surface room temperature phosphorescence analysis	78
4-2. UV absorption (a) and solid surface room temperature phosphorescence (b) chromatograms showing the separation of a mixture containing 200 μ g of phenanthrene and 500 μ g of anthracene pyrene, and benz[a]pyrene. Mobile phase: methanol, flow rate: 0.443 mL/min, sample volume: 20 μ L	84
4-3. Room temperature phosphorescence peak area (I_p) variations of anthracene a., phenanthrene b., pyrene c., and benz[a]pyrene d. with mobile phase flow rate. Mobile phase: methanol. Sample size: 200 μ g of phenanthrene 400 μ g of anthracene. Injection volume: 20 μ L	90
4-4. UV absorption chromatogram of a mixture containing 200 μ g of fluoranthene and pyrene. Mobile phase: methanol, flow rate: 0.443 mL/min, sample volume: 20 μ L	94
4-5. Solid surface room temperature phosphorescence chromatogram of a mixture containing 200 μ g of fluoranthene and pyrene. Obtained under identical experimental conditions of Figure 4-4. Measurement wavelength: 343/385 nm	96
4-6. Solid surface room temperature phosphorescence chromatogram of a mixture containing 200 μ g of fluoranthene and pyrene. Obtained under identical experimental conditions of Figure 4-4. Measurement wavelength: 343/385 nm	98
4-7. (a) Room temperature phosphorescence emission (I_p) spectrum of the three listed compounds using the various excitation wavelengths of fluoranthene (285 nm) (b) Room temperature phosphorescence emission spectrum of fluoranthene obtained under the same experimental conditions as (a)	104

4-9	(a) Room temperature phosphorescence emission (I_{p}) spectrum of the solvent aligned region registered on the maximum excitation wavelength of pyrene (340 nm) (b) Room temperature phosphorescence emission spectrum of pyrene obtained under the same experimental conditions of (a)	10
4-10	Room temperature phosphorescence emission (I_{p}) spectrum of the substrate registered on the minimum phosphorescence intensity observed between the elution of the two compounds. Excitation wavelength: 340 nm	15
4-10	Room temperature phosphorescence emission (I_{p}) spectrum of the substrate registered on the minimum phosphorescence intensity observed between the elution of the two compounds. Excitation wavelength: 340 nm	17
5-1	Solids surface room temperature phosphorescence parameters (I_{p}) emissions of thioxanthone + thiophyllin a and emission a with silica phase flow rate variations. Mobile phase methanol/water 55/45 v/v. Sample size: 500 μ g of each compound. Injection volume: 10 μ l	21
5-2	Solids surface room temperature phosphorescence emission (I_{p}) of thioxanthone (1), thiophyllin (2) and caffeine (3) through filter paper speed: $v = 10$ cm/min, $k = 0.5$ cm/min, $r = 15.1$ cm/min	24
5-3	Optical value sample chromatograms obtained by UV detection and solids surface room temperature phosphorescence detection: (1) thioxanthone; (2) thiophyllin; (3) caffeine. Mobile phase methanol/water 55:45 v/v. Sample size: 500 μ g. Injection: 10 μ l	104
1-4	Room temperature phosphorescence excitation (I_{ex}) and emission (I_{em}) spectra of thioxanthone (a) (a) from optical value samples sprayed on filter paper; (b) after two month storage of filter paper substrate	120
1-5	Room temperature phosphorescence excitation (I_{ex}) and emission (I_{em}) spectra of thiophyllin (a) (a) from optical value samples sprayed on filter paper; (b) after two month storage of filter paper substrate	122

1. 6 Room temperature phosphorescence excitation (laser) and emission (laser) spectra of uric acid in (a) 0.05M sodium uric acid solution sprayed on filter paper, (b) urine and sodium uric acid on filter paper substrate. 111
1. 7 Room temperature phosphorescence excitation (laser) and emission (laser) spectra of uric acid/sodium uric acid on filter paper in the presence of 1M HCl 112

Abstract of Dissertation Presented to the Graduate School
of the University of Florida in the Partial Fulfillment of
the Requirements for the Degree of Doctor of Philosophy

ON THE APPLICATION OF SOLID SURFACE LOW TEMPERATURE
PHOSPHORESCENCE AND ITS UTILIZATION AS A DETECTION TECHNIQUE
FOR HIGH PERFORMANCE LIQUID CHROMATOGRAPHY

By

Andrew Robert Campiglia

August, 1988

Chairman: Dr. James B. Winkler
Major Department: Chemistry

Solid Surface Low Temperature Phosphorescence (SSLT) is an analytical technique that has been growing as a promising tool for the analysis of trace components in biological, pharmaceutical, and environmental samples. Although it is a complex technique to work with than low temperature phosphorescence, the usual sampling procedure which is normally used to perform SSLT analysis is time consuming and therefore, inconvenient for applications in areas where numerous samples are handled routinely.

For example, there have been attempts to develop an instrumental system for the automation of SSLT. In these attempts, the manual steps were eliminated or sped, the solutions were the solid substrates and sometimes the position of the phosphor spot in the sample compartment of the spectrophotometer.

These studies involve the development of a new automatic system which employs a computer interface to speed the analysis solution onto the solid substrates. Since the manual steps were completely eliminated, the new system made SSLT less dependent on the investigator's operation.

short analysis times and satisfactory analytical figures of merit (AFM) shows the applicability of the technique for routine analysis.

The versatility of the new system permitted its use in flowing systems. Flow injection analysis (FIA) was employed as a continuous sample introduction technique in such a way that the tedious elution process involved in batch procedures was substituted by a rapid and easy way of obtaining calibration curves.

The columnless system was then employed as a selective, permanent signal detector for high performance liquid chromatography (HPLC). The chromatographic parameters and the AFM of five well known phosphorescent compounds were compared to those obtained by UV detection. Derivatised compounds were individually identified, demonstrating that the selectivity of the HPLC detector can be a useful feature in case of incomplete separation of complex mixtures.

Finally, the proposed detector was employed in the HPLC analysis of caffeine, theophylline and theobromine. The AFM and the chromatographic parameters obtained with the HPLC detector were compared to those obtained by UV absorption detection. The HPLC and UV chromatograms of spiked urine samples were compared, and the feasibility of keeping an analysed sample on the HPLC paper strip as a permanent record was discussed.

CHAPTER I INTRODUCTION TO PHOTOPHYSICS

Excited State Processes

Photoluminescence spectroscopy is based on the detection of radiation of 100-900 m emitted during the deactivation of electronically excited molecules [1-5]. Under normal conditions, the orbitals of lowest energy of an organic molecule are occupied by pairs of electrons with spins in opposite directions [4]. Since most of the organic molecules have an even number of valence electrons, the resulting electron spins are zero. Such a state, with no net spin, is called the singlet state. The singlet state of lowest energy is known as the ground state, and it is represented in the Jablonski diagram of Figure 1.1 by S_0 . Each electronic state has several vibrational levels which, under different conditions, can represent the energy states of a molecule. At room temperature, most of the molecules are in the lowest vibrational level of the S_0 state.

Through the absorption of electromagnetic radiation (E), a molecule can pass from the ground state to an excited state of higher energy. This transition occurs in approximately 10^{-13} s and results the promotion of an electron from the highest occupied orbital to a previously unoccupied one. If the transition occurs with no change in the spin of the promoted electron, the excited state will have two unpaired electrons with unopposite spins and, therefore, net spin equal to one. An electronic state with these characteristics is known as a singlet excited state. In Figure 1.1, the first and the second singlet excited states are represented by S_1 and S_2 , respectively. If the transition involves a change in the electronic spin, the resulting state will be characterized by two unpaired electrons with parallel spins. In this case, the resultant spin is one, and the excited state involves the name of triplet state. In

Figure 1-1. Afferent diagram showing the different definitions and abbreviations previously; this distinction into a single classification. NE Afferent generation, ISC (Intersecting P phosphorus), VV (ventricular vein) and other abbreviations.

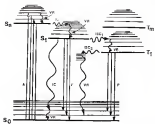


Figure 1.1: The highest state of lowest energy is symbolized by S_0 , while any other excited state of higher energy is represented by S_1 .

When the energy of an absorbed photon is enough to excite a molecule to a state such as S_1 , it usually releases the extra vibrational energy to reach the lowest vibrational level of the state. This nonradiative deactivation mechanism is known as vibrational relaxation (VR) and is in the companion of the energy transfer from the excited molecule to the surrounding medium in the form of thermal energy. Vibrational relaxation involves vibrational levels of the same electronic state, and it is known that any other electronic transition (in the order of 10^{-12} s or less) (1,4).

Through another nonradiative process called internal conversion (IC), the molecule passes from the lowest vibrational level of S_1 to the highest vibrational level of S_0 . This process is the result of the transformation of existing energy into vibrational-rotational energy (3) and occurs between electronic states of the same multiplicity (3). The lowest vibrational level of S_0 is then reached through VR. If the molecule was initially excited to a higher excited state than S_1 , the lowest vibrational level of S_1 would be reached by a succession of IC and VR processes. From the lowest vibrational level of S_1 , the molecule has two ways of directly returning to the ground state. Through IC without the emission of radiation, or by the emission of a photon with no change in the electronic spin. The latter process is responsible for the emission of fluorescence and occurs in a period of time of 10^{-8} to 10^{-9} s. The energy of the emitted photon corresponds to the energy gap between the lowest vibrational level of S_1 and the ground state. When the lowest vibrational level of the S_1 state overlaps with S_0 , the excited state is deactivated by nonradiative relaxation and the emission of fluorescence does not occur.

When the excited photon has the same energy as the one initially absorbed, the process is termed resonance fluorescence. Note that, however, the energy loss is VR and it precedes the emission of

fluorescence at longer wavelengths than the excitation wavelength, and resonance fluorescence is very rare.)

The remaining possibility is access to S_1 from S_0 begins with a process called intersystem crossing (ISC) [10]. ISC is a radiationless mechanism involving systems of different multiplicity which requires a change in the electronic spin [4]. Although this kind of transition has a much lower probability in some than spin-allowed transitions [11,4], the rate ratio of ISC is similar to the one for fluorescence ($10^9 - 10^{12}$ s) and therefore, it competes with fluorescence for the deactivation of S_1 from S_0 ; the molecule can thus pass to the excited triplet state manifold (T_1) and finally, by a combination of VR and IC processes, the lowest vibrational level of T_1 . From T_1 , and through ISC, the molecule can return back to the excited singlet state manifold. Since the triplet states have lower energy than the corresponding singlet states, the transition from S_1 to T_1 requires some additional activation energy. This activation energy can be obtained either by a thermal process or by the absorption of two molecules in the triplet state to produce one molecule in the excited singlet state [4,8]. With the molecule returns to S_1 by the action of a photon, an identical spectrum to the one of conventional fluorescence is obtained [4,8]. This process, which is now represented in the diagram of Figure 1.1, involves the case of delayed fluorescence and has a lifetime of approximately 10^{-4} s.

If instead ISC does not occur, the molecule has two additional possibilities to return from T_1 to S_0 . Through ISC followed by VR, or through the action of quenching in a process called phosphorescence (P). The emission of phosphorescence involves states of different multiplicity and, as a consequence, has a longer lifetime than fluorescence (from 10^{-4} s to 10 s). Since the energy gap between T_1 and S_0 is usually smaller than the one between S_1 and S_0 , phosphorescence occurs in a region of lower energy than fluorescence.

The kinetics of phosphorescence in the basis of the analytical techniques known as phosphorescence, which has been widely applied to the

analysis of compounds presenting phosphorescence emission. Phosphorescence compounds usually consist of molecules with extensive π electron systems. These include a large variety of aromatic molecules either with or without heteroatoms in the conjugated system [1-4]. The free movement of π electrons throughout the delocalized molecular orbitals facilitates the electronic transitions responsible for phosphorescence. For molecules with an heteroatom in the aromatic system, transitions frequently involve the promotion of an electron from a bonding σ orbital to an antibonding σ^* orbital ($\sigma \rightarrow \sigma^*$ transition). Aliphatic molecules, on the other hand, rarely exhibit phosphorescence since the high energy required for $\sigma \rightarrow \sigma^*$ transitions usually causes decomposition prior to excitation [1-4].

Quantum Yield

The intensity of the phosphorescence signal emitted by a compound is determined by its phosphorescence quantum efficiency or phosphorescence quantum yield (Φ_p) [7,8]. This intrinsic molecular parameter is defined as the ratio between the number of phosphorescence photons and absorbed photons. If each absorbed photon produces one phosphorescence photon, Φ_p reaches its maximum value (unity). Most cases, however, there are several deactivation processes that compete with phosphorescence and result in a Φ_p value lower than one. Their effect on the phosphorescence quantum yield is best described in terms of their rate constants. Equations 1-5 relate Φ_p with the rate constants of fluorescence (Φ_{fl}), ISC from S_1 to T_1 (Φ_{ISC}), ISC from T_1 to S_1 (Φ_{ISC}^{-1}), ISC from T_1 to S_0 (Φ_{ISC}^{-2}), and phosphorescence (Φ_p)

$$\Phi_p = \frac{k_{ph}}{k_{fl} + k_{ISC} + k_{ph}} \left(\frac{k_{ph}}{k_{ISC} + k_{ISC}^{-1}} \right) \quad (1)$$

In liquid solutions and gas phase, most of the phosphors have very low Φ_p values as a consequence of the relatively high values of k_{ISC} . By using high viscosity solvents, low-temperature rigid matrices, or solid solutions, the ISC responsible for the transition from T_1 to S_0 can be

continued and, therefore, the value of phosphorescence can be increased.

Lifetime of a Phosphor

The phosphorescence lifetime of a phosphor is defined as the time required for the intensity to decrease to $1/e$ of the original intensity [1,4]. If $I_p(t)$ is the phosphorescence intensity at time t and I_p^0 is the intensity at $t = 0$, τ_p will be given by

$$\frac{1}{I_p(t)} = \frac{1}{I_p^0} \exp \left(-\frac{t}{\tau_p} \right) \quad (2)$$

It is important to distinguish between observed lifetime (τ_p) and intrinsic natural lifetime (τ_p^0) of the phosphor. Observed lifetimes are those obtained under a set of experimental conditions such as solvent, temperature, environment, and physical state of the sample matrix. These experimental parameters affect the radiativeless processes competing with phosphorescence for the deactivation of T_1 and, therefore, no one wants the value of τ_p . The intrinsic natural lifetime can only be measured in the absence of quenching processes, that is, when $k_q \rightarrow 0$. Since radiativeless deactivations are usually present in experimental situations, τ_p^0 cannot be directly determined. However, if the values of τ_p and k_q are known, the intrinsic lifetime τ_p^0 can be obtained [4] by equation 3

$$\tau_p^0 = \tau_p k_q \quad (3)$$

Several phosphors exhibit considerably greater differences in lifetimes than in visible chain composition or emission spectra (for [2] Balin et al., [11] were the first to show that mixtures of phosphors with overlapped spectra could be resolved by time resolution). This method was based on the selection of the proper portion of time between the cut-off of the emission of the sample and the detection of phosphorescence. In fact it was that only the emission from the longer lived compound was detected. Since then several instrumental modifications have expanded the scope of

the method improving the selectivity of phosphorimetry and creating a new technique with the name of laser-resolved phosphorimetry [4].

The Stern-Volmer Effect

The reduction of phosphorescence can be enhanced by the presence of a species of high atomic number (called heavy atom effect) in the environment of the phosphor [3-4]. The heavy atom (HA) can be either chemically attached to the analyte (external HA effect) or independent in the sample matrix (internal HA effect). Between these two effects, the external HA perturbation has been the most used method to improve the sensitivity of phosphorimetry.

The enhancement of the phosphorescence signal by the presence of HA in the environment of the phosphor is the result of an increase in the rates of spin-forbidden processes. This is a phenomenon called spin orbit coupling interaction. The orbital motion of the electrons induces a magnetic field that interacts with the spin magnetic moment changing the direction of the electronic spin [3-4]. As a consequence of the enhancement of the singlet-triplet ISC rate, there is a decrease in the fluorescence quantum yield which results in a decrease in the fluorescence intensity [14]. Thus, the presence of HA can also increase the radiativeless rates of triplet state decay to the ground singlet state [4]; the phosphorescence quantum yield is not always increased and the opposite effect has also been noted [14, 15]. Even thus, however, the phosphorescence decay is more strongly enhanced. To utilize the external heavy atom perturbation causes a decrease in the phosphorescence lifetime of the phosphor which also reduces the probability of collisionless deactivation of the triplet state by collisions [3-4].

Phosphorimetry as an analytical technique

As a means of chemical analysis, phosphorimetry was first suggested in 1951 by Weiss and co-workers [12]. Since then, the technique has grown to become an important tool in the trace analysis of complex processing phosphorescent solution [1, 4].

According to the experimental procedure, phosphorescence can be studied in four different techniques, which include solution (room-temperature phosphorescence [RTP], solid-surface room-temperature phosphorescence [SRTP], nitrocellulose-coated room-temperature phosphorescence [NC-RTP]) and sensitized room-temperature phosphorescence in liquid solutions (sensitized-RTP).

In the first technique, most analyzed compounds have shown, in some extent, a linear relationship between the intensity of the phosphorescence emission and the analyte concentration.

For optically homogeneous and perfectly transparent solutions as the ones frequently tested in RTP, sensitized RTP and certain modified cases, the intensity of the phosphorescence emission (I_p) is related to the intensity of the excitation light (I_0) by the following equation [1, 6]

$$I_p = k_p I_0 - k_q I_0^2 \quad (3)$$

where I_0 is the intensity of the transmitted light. For transparent media, I_0 can be obtained from the Lambert law [4], which is given by

$$I_0 = I_i e^{-\epsilon c l} \quad (4)$$

where ϵ is the molar absorptivity, c is the analyte concentration and l is the thickness of the sample. Equation 3 can then be re-written as

$$I_p = k_p I_i (1 - \epsilon c l) \quad (5)$$

This expression can be expanded in a Taylor series to yield

$$I_p = k_p I_i / (1 + \epsilon c l) = \frac{k_p I_i}{1 + \epsilon c l} \quad (6)$$

For very dilute solutions ($\epsilon c l \ll 1$) and still less the third term in the series expansion can be dropped. The resultant expression is [4]

$$I_0 = I_0 \exp(\mu_p L) = I_0 \quad (10)$$

which shows the direct proportionality between I_0 and α .

For optically homogeneous and non-transparent solids, the applicability of Lambert Law has some limitations [2-4]. In EPR measurements performed on solid substrates (SEPP) or non-like matrices (matrix EPR cases), both specular and diffuse reflection are extensively observed. In addition, the emission reflection can be matched by the solid matrix as well as the analyte. Any theoretical model employed to derive an expression relating intensity and concentration must take these effects into consideration.

Isidoro and Rush proposed a set of differential equations of the first order in which the complex process of light propagation inside homogeneous scattering media is characterized by only two coefficients (24,17). Although this model is based on several restrictive assumptions that are not frequently fulfilled in experimental situations, its simplicity has allowed approximations in deriving the formulas for more quantitative studies [4]. Benninger and Warburton [17] utilized a modification of the Isidoro-Rush differential equations to obtain an expression for the phosphorescence intensity emitted in non-like matrices and crystal glasses. At low concentrations of analyte, the intensity of phosphorescence is given by

$$I_0 = 14.4\mu_p L^2 \left(\frac{1}{1+\alpha L} \right)^2 = 14.4\mu_p \left(\frac{L^2}{1+\alpha L} \right) \quad (11)$$

where

μ = fraction of radiation absorbed per average path length

($\mu = 2.303 \alpha L$)

L = average cell path length for diffuse reflectance, cm^{-1} , and

α = fraction of incident radiation absorbed per path length, cm^{-1}

(α = function of analyte concentration)

If the scattered light is negligible ($\alpha L \gg 1$) equation 11 reduces to

$$I_0 = 2k_p k_2 \bar{B} + 4 + 2k_p k_2 \bar{B} \quad (10)$$

In high analyte concentrations, the intensity of phosphorescence emission is given by

$$I_0 = 2k_p k_2 C \frac{\sqrt{K}}{\sqrt{K} + \sqrt{B}} \quad (11)$$

If k is k_2 , equation 11 reduces to

$$I_0 = 2k_p k_2 \sqrt{\frac{K}{B}} \quad (12)$$

If k is k_1 , I_0 is then given by

$$I_0 = 4k_p k_1 \quad (13)$$

Equations 10 and 11 show that the analytical curves (log I_0 vs log c) in heterogeneous diffusely reflecting media should have a slope of unity and zero at low and high concentrations, respectively. These theoretical expressions were successfully supported by experimental results obtained at low temperatures [17]. In most cases, however, the same behavior has been observed in ESR, where the relaxing and reflecting media consist of solid substances [5].

Until 1975, most work involving phosphorescence was carried out at low temperatures [27-30]. By the use of cryogenic equipment, the solutions were frozen in both a rigid matrix to eliminate the collisions competing with phosphorescence for the deactivation of the triplet state. Since then, very little has been done in the area of EPR. The lack of widespread use can be attributed to three major reasons [31-33]. The high cost of cryogenic equipment and liquid coolant, the time-consuming deaeration of the solution to avoid quenching effects, and the cumbersome procedure to introduce the sample into the cooling system. Two kinds of detectors (GEM (gas-filled metal) cathode tubes with either Union Carbide tubes [34] or ^{63}Ni or ^{57}Co foil change in surface concentration), and relative standard deviations [35] of measurements

Sampling from 1 to 10, were only obtained with clear glasses extracted. Variations in the rate of sample testing caused modifications in the final result, depending either in a stained glass or in a new. In addition, the soil packaging had to be carefully performed to reach good reproducibility in such a way that the presence of a skilled technician or chemist was necessary to obtain satisfactory results. These problems turned LIT into an inconvenient tool for routine analysis of a large number of samples.

Around 1970 to 1973, Scholman and Walling [40-42] reported the observation of strong phosphorescence emission from a wide variety of basic organic compounds adsorbed on solid substrates. Filter, aluminum paper, asbestos, and glass fiber were employed to provide the rigidity required to restrict rotational quenching and to prevent radiationless deactivation of the triplet state. In contrast to LRF the coupling procedure was very simple and required no more than 10 min per sample. Following these early reports, a large number of studies dealing with the optimization of parameters affecting the sensitivity and reproducibility of HETP have appeared in the literature. Depending on the analyte, solid surface, and experimental conditions, calibration curves with IEF of 10^4 to 10^6 fold change in analyte concentration, IEF is the sensitivity or integration factor, and RSD (ranging from 1 to 15%) can be easily obtained. The simplicity of the coupling procedure; elimination of the need for cryogenic equipment, and the possibility of automation have turned HETP into the most popular phosphorescence technique of the last two decades [20].

Alkali-stabilized zinc-hydroxide phosphorizing in aqueous solution [21-24] can also applied as an analytical method of analysis by Elina Lew and co-workers [25,26]. The method was employed to determine a wide variety of phosphors including borates, nitrogen oxides, hydroxyl zinc phosphide, nitrate, and compounds of pharmaceutical interest. Analytical solutions consist of colloidal suspensions of colloids or detergents which reduce the characteristic coloration

of the analytes from external standards and vibrational spectroscopy. The application of surfactants only serves stress a certain concentration known as critical micelle concentration (CMC). This concentration depends upon the chemical structure of the surfactant and the nature of the solvent. In order to obtain satisfactory results, the CMC value of a particular surfactant has to be determined before its use. If no data are available in the literature, the CMC determination can be performed either by titrimetry or by fluorescence titration of a probe compound [13-15]. The main disadvantage of the technique, however, is the necessity of thorough sample desorption, which results in a sample analysis time of approximately one hour, restricting the use of HPLC in routine analysis of a large number of samples [14]. There are, nevertheless, considerable advantages in the use of the alcohol method. In most cases, the sensitivity and precision of HPLC are comparable to those obtained by LTP [16]. The HPLC analysis of large polycyclic aromatic compound compounds in aqueous solutions is facilitated by the high solubility of this species in the mobile environment, and finally, the alcohol approach offers a means to conduct phosphorescence analysis that can be directly applied to flow systems and liquid chromatography detection [14].

HPL detection in continuous flow and chromatographic systems can also be performed by means of modified HPL [13-16]. In these techniques, the weakly or non phosphorescent analyte (donor) transfers its triplet energy to a given acceptor. A suitable acceptor should have a triplet energy lower than that of the donor, a high quantum phosphorescence yield, and a lower molar absorption in the excitation region of the donor. In addition, the energy gap between the triplet states of the donor and the acceptor should be enough to prevent significant reverse radiation. In fact, the most appropriate acceptor found for the technique has been fluorescein (FAC) [18]. 126 in the emission range were obtained by flow injection of several polyhalogenated naphthalenes and biphenyls and liquid chromatography analysis of mixtures of chlorinated naphthalenes, biphenyls, and dibenzofurans [19]. According to the authors [18, 19]

several advantages justify the use of sensitized RPL as a detection technique. Even though sensitized RPL is based on an indirect technique, it is inherently more sensitive than IR-absorption; the background noise due to scattering and fluorescent impurities is negligible at the selected wavelength of RPL (532 nm) and it is particularly selective since all of the constituents of a sample do not produce the sensitized phosphorescence signal of the acceptor. Further research, however, is necessary to develop new acceptor systems and assess the application potential of sensitized RPL to other kinds of compounds.

CHAPTER 2
EXPERIMENTAL CONSIDERATIONS FOR
SOLID SUBSTRATE ROOM TEMPERATURE PHOSPHORESCENCE

Even though Kohn [36] was the first to report the use of collisions as a rigid matrix to enhance the phosphorescence emission of several compounds at room temperature, the potential of RHP as an analytical technique was only recognized after the studies performed by Schuler and Walling [38,39]. When adsorbed on solid substrates such as paper, cotton, cellulose substances and glass fiber, the luminescence of a wide variety of polycyclic aromatic hydrocarbons, aliphatic aldehydes, phenols, and various aromatic naphthalene phosphorescence intermediates is shown enhanced by the same compounds at RHP temperatures [38,39]. At room temperature, the emission signals were obtained on filter paper. The coupling procedure was very simple. Paper or signal detection, known as a filter paper strips were saturated with the analyte solution and slowly dried under an infrared lamp to avoid the presence of humidity, which showed to be a quencher of the phosphorescence signal. The presence of oxygen, which is a serious phosphorescence quencher in solution measurements, did not show significant effect on the RHP signal of most studied compounds. The fact that no phosphorescence emission was detected from freshly ground samples of pure solids or from the corresponding crystals grown from solutions of the organic solids led the authors to conclude that the matrix slightly necessary in the emission of strong phosphorescence was obtained via absorption of the molecule in the surface of the substrate [38,39]. Since at room temperature phosphorescence was observed from molecular compounds, it was also suggested that the loose state of the molecule imposed the rigidity of the matrix and released, as a consequence, the collisional deactivation mechanism of the excited state [38,39].

The direct application towards the analytical usefulness of the phenomenon was reported by Winklerhorst and co-workers [11,22]. Great care was taken in developing a rapid and reproducible method to determine small amounts of acid derivatives of naphthalene [21] and compounds of biological interest [23]. By using a microinjection syringe, 1 μ l of a 10 mM solution of the desired analyte were applied to Whatman 403 Filter paper discs... however, drying methods (including oven and air blower) also drying followed by a period in a desiccator, and infrared lamp were assessed for best results. In the analysis of acid derivatives of naphthalene [20], the more reproducible and strong signals were obtained by air drying followed by a period in a desiccator. This procedure, however, was time consuming and involved more sample handling than desired. Heating the sample by means of an oven or a hot air blower proved to be too destructive for the analyte and the substrates [11,20]. Infrared lamp, though, showed to be both gentle and effective [20]. 100 in the temperature level and calibration curves between one and four orders of magnitude were easily obtained in an analysis time of approximately one minute per sample [22]. In agreement with the original assumption that the basic strength of the phosphor was directly related to the induction of RTP on solid substrates [10-15], variation of phosphorescence from nonfluorescent compounds such as polycyclic hydrocarbons (PHHs) was not observed [22]. Relatively strong phosphorescence, however, was detected from some uncharged species such as nifedipine and 5-norpi-veratril according to the authors [22]; this anomaly was indicative that hydrogen bonds rather than Lewis interactions were involved in the induction of RTP. Hydrogen bonding between the phosphor and the hydroxyl groups of the Filter paper was then suggested as one of the possible mechanisms to avoid radiationless deactivation of the triplet state [20].

In order to further investigate the nature of the surface-phosphor interaction which results in the observation of RTP, Ishizawa and Ficker [22] studied the phosphorescence signal of 4-hydroxynaphthalene and sodium 1-naphtholate at room temperature. The analytes were applied on

several supports of different polarity. Strong visible phosphorescence was observed from all substrates regardless on abundance of surface hydroxyl groups such as paper, cationic, anionic, and 99% HTP polyethylene fiber. No paper bind. An appreciable phosphorescence, however, was noted from supports consisting few or no surface hydroxyl groups such as HTP polyethylene fiber, borosilicate glass fiber, paper, or cationic bind. In addition, a reduction of 94% in intensity was noted when the phosphorescence signal of 1-naphthol adsorbed on cationic Styrene No. 1 filter paper was compared to the one emitted by the same compound adsorbed on filter paper with an anionomer. The treatment, which was performed by the immersion of the filter paper in diethylaluminumchloride, covered most of the hydroxyl groups from the surface of the substrate. According to Ishizawa and Fisher [11] the replacement of a polar or basic compound combined with the necessity of a support with no hydroxyl groups strongly indicated hydrogen bonding as the primary mechanism of adsorbing HTP cations on solid substrates. Supporting evidence for this kind of interaction was also provided by van Veenendaal and Nienhuise [14, 15]. In the search for a new substrate for HTP, they observed strong phosphorescence emission from p-aminobenzoic acid (PABA) adsorbed on cationic anionomer (BAAn) [14]. The mode of adsorption of PABA on the substrate was then investigated by infrared (IR) spectroscopy [15]. By comparing the IR spectra of PABA, BAAn, and PABA adsorbed on the substrate, it was noted that the N-H stretching vibrations of PABA at 3300-3450 cm^{-1} disappeared in the spectrum of the phospor adsorbed on BAAn. The fact was attributed to hydrogen-bonding between the amino group of PABA and the carboxyl groups of BAAn. The N-H vibrations were probably shifted to a spectral region of longer wavelengths and overlapped by the broad methyl stretch band of BAAn at 2800 cm^{-1} [14]. Additional hydrogen bonding evidence was later reported in HTP studies involving a large variety of nitrogen heterocycles and aromatic amines adsorbed on silica gel and polypropylene acid-alkali anionomer [16-21]. Both kinds of substrates contain surface silan for potential hydrogen-bond formation.

The analyses were repeated from neutral, acidic and basic solutions and each supports and the relative phosphorescence intensities were compared. In general, analyses repeated from acidic solutions produced the greatest signal intensities. These IR results confirmed the formation of hydrogen bonds between compounds and cellulose. Strong phosphorescence emission, however, was also detected from compounds incapable of forming hydrogen bonds with the cellulose [10, 11], suggesting that other mechanisms than hydrogen bonding are involved in the emission of phosphorescence at room temperature.

For the specific case of compounds adsorbed on cellulose paper, a viable luminescence mechanism for ECP luminescence has been recently proposed [14]. The mechanism is based on inherent properties of the cellulose Cellulose undergoes considerable swelling in the presence of polar agents such as water and ethanol which use the same common solvents employed in EPRP analysis. The swelling causes a new stress in the paper fibers facilitating the entry of phosphor molecules into micromolecular pores. When the substance is dried, the cellulose fibres collapse and the phosphor molecules become trapped between the cellulose chains. As a consequence, the molecular vibrational motions responsible for nonradiationless deactivation of the triplet state are restricted; the phosphor is protected from quenching by molecular oxygen and an enhancement in the ECP signal is observed [14]. This mechanism was evaluated by studying the behavior of the phosphorescence signal of 4-biphenylcarboxylic acid (4-BPCA) and 4-aminobenzonitrile (4ABN) adsorbed on Whatman No. 1 MM chromatography paper. Prior to analysis deposition, the substrate was exposed with solvents of different polarity such as hexane, acetone, propanol, ethanol, methanol, and water. Hexane and acetone did not swell the cellulose fibres but the other four solvents swell the substrate by loosening sides from propanol to water. It was observed that the 4BPCA samples exhibited an appreciable intensity when prepared in nonswelling media. On the other hand, the ECP intensities of 4BPCA samples prepared with the polar solvents were significant and increased in

the strict order of nuclei swelling. The same trend was observed for the methyl samples except that the phosphor displayed significant intensity when prepared with benzene or acetone. The polar solvents, though, produced much higher EPR signals than the nonpolar solvents. Further information was provided by comparing the phosphorescence intensities of monopills and biopills compounds adsorbed on cellulose previously exposed with water [6]. Small small molecules supposedly penetrate cellulose more easily than large ones, stronger phosphorescence emission was expected from monopills phosphors. The expectations were confirmed, suggesting that not only cellulose swelling but also nuclei function play an important role in the luminescence of phosphor molecules on paper substrates [16]. It is important to mention, however, that the comparison between the phosphorescence signals of monopills and biopills compounds was made without taking into consideration the phosphorescence quantum yields of the studied compounds.

Although a great deal of effort has been focused on understanding the mechanism responsible for the emission of room temperature phosphorescence on solid substrates, it has not yet been possible yet to provide a logical foundation for the development of new EPR methodologies. In short, the selection of appropriate substrates and best experimental conditions for EPR detection has been based on information obtained from previous analysis. If data are not available in the literature, the optimization of parameters is usually performed on a trial and error basis which involves time consuming procedures. Once the method is developed for a particular analysis, though, phosphorescence data are fast and simple to acquire. Simplicity of experimental procedure, sensitivity, relatively small sample requirements and low cost are advantages that have induced the technique into an attractive tool for the analysis of compounds of diversified interest [7-10].

Quenching Effects

The phosphorescence intensity emitted by compounds adsorbed on solid substrates may be decreased or even quenched by interactions with other

chemical species [4]. One of the most efficient triplet quenchers for molecular oxygen [4]. Interaction of triplet state oxygen (the natural ground state of oxygen) with a molecule in an excited triplet state results in the collisionless deactivation of the excited molecule and the production of excited singlet state oxygen [7]. Although the presence of oxygen in HPLC is not as critical as it is in ESR detection measurements [2,4], it can cause to some degree quenching of phosphorescence emission. Scholten and Burke [10] studied the oxygen effect in the phosphorescence signal of NADPH₂ adsorbed on filter paper disks. A reduction of approximately 30% in emission intensity was noted when the phosphorescence signals of samples exposed to dry oxygen for 15 minutes were compared to those measured under a flow of dry oxygen. Baskin and co-workers [11] observed a reduction of 5% in the phosphorescence emission of pyrene when the intensity measured under an oxygen atmosphere was compared to the one detected under a flow of dry nitrogen. Similar behavior was noted by Jones and Kinschtein [14] in the study of several polycyclic hydrocarbons. Reductions ranging from 10% (pyrene) to 15% (phenanthrene) were verified when the ESR detection characteristics of samples measured under dry air were compared to those obtained under nitrogen or oxygen atmospheres. Such strong oxygen quenching effects, however, were not reported for highly polar compounds. When Fuli was spread on Elinor paper and subjected to dry air, oxygen and nitrogen flows, similar phosphorescence intensities were observed [16]. Strong ESR emission was still detected from methionine salts, however, that are completely adsorbed on silica gel columns and measured under a flow of dry air [3]. The presence of oxygen in dry air, however, quenched the ESR emission of nitrogen homocyclopentyl adsorbed on silica gel and Elinor paper [17]. Furthermore, it was noted that the ESR of compounds adsorbed on silica gel was generally more subject to oxygen quenching than the ESR of the same compounds adsorbed on Elinor paper. The percent enhancement of benzil(1)anthracene measured in bottom versus air, for example, was 3% for silica gel and only 1% for Elinor paper. According to the authors [17]

11
this seemed reasonable since either gel or more porous than filter paper
and therefore has more surface area on which copper could potentially
adsorb with adsorbed compounds. The influence of copper atmosphere here
sample matrices used in HRF was also studied by Riley and Deyhoid [18].
The phosphorescence lifetime of 2-naphthol was enhanced on filter
paper was increased by coating the substrate with substances such as
 CH_3COOH , H_2SO_4 , NaF , H_2O , glycine, glucose, and sucrose. The HRF
intensity was enhanced by the presence of moisture, but the effect of other
substances was less predictable and needed further investigation. The
authors [18] suggested that the added substances could be plugging up the
channels and intersections of the matrix, decreasing the permeability to
copper. In addition, these materials could layer a slightly on the
substrate and inhibit specific internal surface responsible for
collisions/deactivations of the excited state. An opposite effect to
the one observed by Riley and Deyhoid [18] was obtained when HRF
measurements were performed under humid conditions. Using paper as a
sample matrix, Johnson and Parker [11] demonstrated that copper
quenching occurs much more slowly in the presence of moisture. The
efficiency of copper quenching in the HRF emission of $\text{Cu}(\text{NH}_3)_4^{2+}$ increased
dramatically as the relative humidity of the copper atmosphere increased.
The authors [11] suggested that moisture could be disrupting hydrogen
bonds between phosphor and substrate, facilitating the transport of
copper ions into the vicinity of the phosphor. The presence of moisture itself
has proved to be an extremely powerful quenching agent of HRF emissions
[19-21, 23-25-26]. Further facilitating the interaction between copper and
analyte, water molecules might compete with the phosphor for binding sites
on the support, thus decreasing the analyte-support adsorption process and
lowering the probability of collisions and vibrational quenching. For
analyte HRF emissions, therefore, it is recommended to dry the sample
prior to insertion and keep it dry during the measurements. Several
methods have been employed in the drying step [4]. One of the most common
is the use of an infrared heating lamp. This method is rapid, convenient

and generally nondestructive for both the sample and the substrate between 1 and 5 minutes are required in dry nitrogen or dry oxygen, and the drying temperature can be set by adjusting the distance between the sample and the lamp. The phenomena of sublimation during the measurements can be easily avoided by passing a gentle flow of dry nitrogen or dry oxygen through the sample compartment of the spectrophosphorometer. The lowest gas is usually dried by passing it through one or two drying cartridges filled with calcium sulfate and placed prior to the inlet of the spectrophosphorometer.

Background Influence on LOD

The sensitivity of an analytical method is usually evaluated in terms of limit of detection (LOD). The value of the LOD is directly related to the smallest amount that can be detected with reasonable certainty [48]. According to the International Union of Pure and Applied Chemistry (IUPAC) [49], the smallest detectable signal (s_d) is given by the following expression:

$$s_d = \bar{s}_b + k s_b \quad (14)$$

where \bar{s}_b is the mean average of the blank responses, s_b is the standard deviation of the blank measurements, and k is a statistical factor chosen in accordance to the confidence level desired [48]. From equation 14, it can be seen that the lowest s_d values (and s_d) are obtained for the lowest signals of analytical blanks. Therefore, in order to obtain the highest detection power with a specific analytical method, it is convenient to reduce the blank signal to the minimum possible value.

In ESRF measurements of solutions of pure compounds, the analytical blank signals are obtained by measuring the phosphorescence emission of solvents spread on solid substrates. In most ESRF determinations, relatively pure solvents are used and the main contribution to the phosphorescence background is usually given by the solid substrate. As with other analytical methods, low ESRF detection limits are obtained with low background signals. As a consequence, many materials have been studied to find a substrate with low phosphorescence emission between 300

and 444 nm, which is the spectral region where most compounds phosphoresce. In addition, a suitable HPLC solvent should possess the versatility to enhance, as much as possible, the HPL signal of a wide variety of phosphors with different physico-chemical characteristics, among the materials investigated cellulose and particularly filter paper, appears to be the most convenient substrate for the technique [4, 12, 18-22]. The main advantages of cellulose over other materials are low cost, simplicity of handling and availability of a wide selection of different papers enabling one to select the best substrate for phosphors with diverse characteristics. Nevertheless, several problems are related to its use in HPLC. Sensitivity is subject to changes, depending on the surface and variation in the physical and chemical composition within the same batch can deteriorate the reproducibility and sensitivity of measurements [4]. However, the major drawback is the broad fluorescence bands of excitation spectra from 260 to 440 nm, and phosphorescence spectra from 375 to 675 nm [24]. This background phosphorescence interferes, which is often of the same order of intensity as the analyte signals from relatively high analyte concentrations, severely limits the sensitivity of HPLC [25]. Various modifications, or even irregular metal screens, have been suggested as possible sources of the background signal [26]. Several strategies have been used to decrease this signal, to some extent, using solvent collection, or chromatography coupled to laser treatment, or signal background subtraction with the help of a computer assisted spectrofluorometer, by Kluenderhof and co-workers [26-32]. The most significant improvements, however, were obtained by ultraviolet irradiation treatments [33,34]. Martinez and Bojop [34] observed a reduction of 10% in the phosphorescence intensity of filter paper irradiated at 255 nm for 27 hours in the sample compartment of the spectrofluorometer. The idea of ultraviolet treatment was later refined in a modification proposed by Campiglia and Solina [35]. Sheets of filter or chromatography paper were water saturated in a waterbath apparatus for 4 hours, irradiated with quartz tubes and exposed to

ultraviolet radiation for the same period of time. The ultraviolet treatment was carried out in a photobiological reactor equipped with five lamps with λ_{max} emission at 254 nm and seven with λ_{max} emission at 366 nm. A 744 background reduction was obtained, which allowed the phosphorescence lifetime for 2,4,6-trichloro-1,3,5-triazine (1 mg/100 g) 2-methyl-2-naphthol and 1-naphthol to be obtained. Since the low background signal remained constant for several weeks after treatment, the strips of paper could be stored in a desiccator to be conveniently used in routine analysis.

Internal Heavy-Arson Filter

The sensitivity of an analytical method can be improved not only by reducing the intensity of the analytical blank but also by increasing the analyte signal. As discussed in Chapter 1, the phosphorescence selection of compounds adsorbed on solid substrates can be greatly enhanced by the presence of heavy-arsens in the sample matrix. Inghel and White were the first to report on the internal heavy-arsen effect in HRP [30]. They observed an increase of about 40 times in the phosphorescence intensity of 1-naphthol-2-sulfonate when 1.8 x 10⁻³ M was spread on the filter paper containing the analyte. Further results were obtained for 1-naphthol-2-sulfonate, 2,3-naphthol-2-sulfonate, 2,4,6-trichloro-1,3,5-triazine, 2-naphthol, 2-naphthol-1-sulfonate, and 2-naphthol-1-sulfonate. Inghel and White extended the use of iodine as an internal heavy-arsen partner to the HRP analysis of a wide variety of compounds of biological and pharmacological interest [31]. The analyte solutions were prepared in 10 mM-10 mM HCl (1:1), spread over filter paper discs and dried for about 10 minutes by infrared lamp heating. The heavy-arsen enhancement factor, which was defined as the ratio of the analyte phosphorescence signal in 10 mM-10 mM HCl (1:1) solution to that in 10 mM aqueous solution, ranged from 1.8 to 1000 for quinine, and 40 for erythrosine. In some cases, the 400 were reduced by one or two orders of magnitude, showing the above range of using iodine to improve the sensitivity of HRP. Comparison on fluorescent iodine, though, were not observed when HCl was employed in the analysis of aromatic compounds. In the study of the phosphorescence

behavior of anthracene, pyrene, phenanthrene, benzo(a)pyrene and acenaphthene. He [18] and co-workers [19] noted that the voltages of the in basic solutions of these compounds featured only weak phosphorescence signals. The use of silver chloride, however, considerably enhanced the phosphorescence intensities of neutral solutions of phenanthrene and pyrene. For these two phosphors, LOD in the nanogram level were obtained, opening up new possibilities for the AETP analysis of complex compounds. The effect of a variety of heavy-metal ions on the AETP signal of rhodamine was later reported by Jaisankar [24]. Solutions of salts of thallium, lead, thorium, cerium, etc. were employed to coat filter paper strips prior to chemical separation. After drying the substrate for 15-25 minutes with an electric blower at room temperature, an alcohol solution was spotted on the filter paper strips and dried for 10 minutes in an oven at 200°C. The highest enhancements were observed with lead acetate, thallous fluoride and thallous acetate. By employing a 0.16- or 1.6 solution of lead acetate, amounts of rhodamine as low as 30 µg were successfully measured, and calibration curves with LOD between 0.005 ± 0.1 µg were obtained. Lead (II) and thallium (I) were also employed to enhance the phosphorescence emission of folic acid on filter paper. Lee Yee and Vinsantorn [25] selected AgNO_3 , $\text{Pb(NO}_3)_2$, HgCl_2 , $\text{Hg(NO}_3)_2$ and $\text{Hg}_2(\text{CH}_3\text{COO})_2$ to study the heavy-ion effect on the phosphorescence emission of styrene, toluene, 1,2,3,4-tetraacetylmorphine, fluorenone, and pyrene. Of the heavy ions, thallium (I) seemed to be the greatest enhancer of AETP signals for all ions with the trend being $\text{Tl}^{+} > \text{Ag}^{+} > \text{Pb}^{2+} > \text{Hg}^{2+}$. Based on the enhancements observed, the authors [24] estimated that the LOD of the studied compounds could be lowered up to 5-fold by using thallium (I) salts. Not only the sensitivity but also the selectivity of AETP can be improved with the presence of heavy ions in the sample matrix. Verheek and Boeyens [26] proposed the use of different heavy-ion salts to determine target compounds in complex mixtures without previous separation. The ion sequence, which was called selective mineral heavy-ion pre-formation (SEMHP), was based on the fact that preferential

enhancement by various heavy ions of some stronger signals observed with ions that do not enhance. EDAP was applied to the qualitative and quantitative analysis of several mixtures (up to seven components) of polynuclear aromatic compounds of environmental and biological importance. Among the heavy ions with which the highest EFP enhancements were obtained with AgBr₃, GaI₃, BaI₃, BaBr₃, Ph₃IBr₃/Ph₃Br₃ and UO₂²⁺. Since these counterions could have an effect on the EFP enhancement factor, a previous determination of their optimum values for maximum EFP emission was performed by measuring the phosphor-organic signal of analyte solutions at several heavy-ion concentrations. Three characteristic ranges were observed. At very low concentrations (less than 10⁻³ M), the amounts of heavy-ions present in the sample spot were insufficient to induce significant phosphorescence enhancement, at medium concentrations (more than 10⁻³ M) EFP increased with heavy-ion concentrations, at high concentrations some saturation effects occurred and the influence of heavy-ion amounts no longer caused any substantial increase in the EFP signal. Additionally, though did not depend only upon the absolute concentration of heavy ions but also upon the relative ratio between heavy-ions and analytes. The saturation condition, which corresponded to the maximum EFP enhancement, was obtained at high heavy-ion concentrations and sufficiently low analyte concentrations. These most heavy-ions were used (their reliability values at 0.1-1 M concentrations range) analyte concentrations lower than 10⁻³ M could be measured to satisfy the requirements for detection. This fact, however, did not in present any limitations for analytical programs because most EFP researches deal with sample solutions within 10⁻² - 10⁻³ M ranges. The highest phosphorescence enhancements were obtained with 0.1 M AgBr₃, 0.1 M GaI₃, 0.2 M BaI₃, 0.1 M BaBr₃, 0.1 M Ph₃IBr₃/Ph₃Br₃ and 0.05 M UO₂²⁺. By selecting the appropriate combination of heavy-ion solution and emission wavelength, the authors [26] were able to perform the analysis of specific target compounds with practically no interference from the other constituents of the mixture. Most compounds measured were in the

nanogram level range, showing the potential of HRP as a useful tool in the HRP analysis of substances without previous separation. The internal heavy atom effect has also been applied to the HRP determination of several pharmaceutical compounds (94-97), pesticides (98), antibiotics (99), and pesticides (94-95, 97). In most cases, the presence of heavy atom has successfully improved the sensitivity of the analysis allowing a 100 to 1000-fold increase in the nanogram-gram range.

The effectiveness of heavy atom perturbations can be increased by the presence of surfactants in the matrix of the phosphor. Bellam and co-workers (100) were the first to demonstrate the advantage of using surfactants in HRP. They studied the effects of sodium and silver acetate, sodium stearate and silver lauryl sulfates (TDS, AgDS) potassium laurate and sodium lauryl sulfate (SLS) on the phosphorescence intensity of carbonyl. Three μ l of analysis ethanolic solution (10 μ g/ml) were spotted onto filter paper discs, dried under a stream of nitrogen for 30 minutes and their HRP signals measured (1,). Subsequently, 3 μ l of the heavy atom enhancer solution were added to the same spot and the drying and measuring procedures were repeated (1,). The enhancement factors (I_p/I_0) varied from 1-8 to 12, depending on the type and amount of enhancer used. Although the SLS ethanolic does not contain a heavy atom, a 1-8-fold enhancement factor was observed. According to Bellam et al. (100) the presence of SLS on the surface of the paper could provide other sites of interaction for the phosphor resulting in increased rigidity of the molecule etc. Therefore, higher intensity of the phosphorescence solution. The enhancement factors of the laser concentrated solutions (0.005 M) of TDS and AgDS were higher than those observed from similarly concentrated solutions of 0.1 AgDS or TDS, a comparison of the 0.1 M AgDS and TDS with their corresponding control value showed increased intensity in the net phosphorescence signal of 3.3 and 1.8 respectively. In addition, it was observed that an increase of the concentrations of the surfactant salt in the spraying solution had a marked effect on the intensity of the phosphorescence when the concentrations of AgDS and TDS were increased.

from 0.00 M to 0.01 M, a 1.5-fold increase in the intensity of cadmyl was obtained. A similar increase of silver and thallium only produced an 1.1-fold increase in the intensity. At 0.01 M concentration, the net phosphorescence signals in the presence of the surfactants silver were higher by a factor of 1.2 and 5.1 for silver and thallium, respectively. In order to obtain a better understanding of the reason for the observed phenomena, x-ray photoelectron spectroscopy (XPS) analysis of the sample was performed. The XPS data revealed that both TlPI and AgPI were better retained on the surface of the paper than their corresponding chlorine salts. According to the authors [41], this was indicative that the observed phenomena could be attributed to the increased availability of the heavy-ion cations at the surface of the substrate, which probably facilitated the increasing heavy-ion and phosphor interaction. Since the long hydrocarbon chain of the surfactant could avoid the penetration of phosphor molecules into the cellulosic paper and increase their interaction with heavy-ion at the surface of the substrate, Bellon et al. [42] suggested that higher RFP enhancements could be obtained if AgPI or TlPI solutions were sprayed on the paper prior to the phosphor, or if a pre-treated solution of the phosphor with AgPI or TlPI was utilized. The use of surfactants in RSTP was later suggested by Randa-Ramos et al. [43] in the analysis of arsenic, lead and cadmium. The influence of the surfactant character on the RFP signal of complex compounds was studied by employing *n*-octyl as a model compound. Bellon decetyl sulfate (BDS) and tetris decyl sulfate (TDS) were selected as anionic surfactants. Not only was the positive species and *n*-decyltrimethylammonium chloride (TDA) was chosen as the cationic surfactant. The highest phosphorescence signals were observed by spraying on filter paper films previously covered with 0.02 M TiPO_4 , a mixture of the samples dissolved in heptane with an aqueous solution of the surfactant. The highest enhancements factors were obtained in the presence of BDS (4.4) and TDS (3.7). A dramatic intensity reduction was observed with the other two surfactants. In the case of TDA, the

spectrum of the analyte disappeared completely. As a possible explanation, Davis, Kiser and coworkers [10] suggested that the higher affinity between the analyte and the sorbent coefficient tube increased the probability of intermolecular between phosphor activation and quenching ions. In addition, excitation of sorbent analyte with the surfactant would aid the migration of such species inside the submicroscopic pores of the cellulose fibers to produce a better arrangement of the analyte and reduce radioluminescence deactivation of the triplet state. By using a 24 mM solution, all studied compounds showed LOD in the subnanogram level. Then their values were compared to those obtained in the absence of the surfactant, an improvement factor of 1-18 M was verified. LOD in the subnanogram level were also obtained for PAHs and phenanthrene derivatives [26]. The analyte solutions containing 10 mM were sprayed on ELNEX paper films previously treated with 0.1 M TMS₂. Before measurement, the samples were dried for 10 min in an oven at 110 °C and for 10 min in the sample compartment of the spectrofluorimeter under a flow of dry nitrogen. The order of addition of reagents on the filter paper was modified in studies performed by Kiser and coworkers [21,22]. A methanol solution of quinine lauryl sulfates (TMS) was employed in the HPLC analysis of anthracene [23] and several PAHs [24]. The TMS solutions were spotted on the paper substrates prior to analyte deposition. In both cases [21,22], it was observed that the highest RFP enhancement was obtained with TMS concentrations ranging from 5 mM to 5 mM M. For these concentration ranges, the net phosphorescence signal of anthracene with TMS was double the one observed with TMS₂. For all analytes studied, the LOD were in the nanogram level and compared favorably with those in literature reports, which involved a variety of filter papers and matrix modifications. According to the authors [24], these studies suggested that filter paper previously treated with TMS could be used as a general method for trace analysis of different kinds of PAHs. The substrate can stable over a long period of time, meaning it could be prepared ahead of time and stored for future use in routine analysis.

CHAPTER 1

AUTOMATIC SAMPLING SYSTEM FOR KREEP ANALYSIS

Introduction

Although KREEP is a simpler technique to work with than low-temperature phosphorescence, the individual sampling procedure which is usually used to perform KREEP analysis is time consuming, and therefore inconvenient for applications where numerous samples are handled routinely. In addition, the several manual steps involved in sample preparation can lead to appreciable random errors which affect the reproducibility of the technique.

Two attempts have been made to reduce the manual steps and the sampling time involved in KREEP analysis [42, 43]. Ye-Roth and co-workers [42] designed an automatic phosphorescence system coupled to an Adair-Brown quartz fluorimeter with the sample compartment modified for detection of phosphorescence. A laboratory constructed rotating mirror assembly was employed to withstand the disturbances of fluorescent excitation and emission scattered light to the detection of KREEP signals. The collimated light beam from the excitation monochromator was reflected by the mirror onto the surface of the substance, which rested horizontally across the slit located at the top of the sample compartment. By rotating the mirror to the emission monochromator, the phosphorescence signal emitted from the sample was reflected to the detection system. Glass fluorescent lifetimes (10^{-8} - 10^{-6} s) are much shorter than phosphorescence lifetimes (10^{-2} - 10 s); the possible collection of fluorescence from the sample was no longer present at the onset of KREEP detection. The scattered light was greatly reduced by inserting the rotating mirror into the Adair-Brown phosphoroscope. Samples were

specimen drop by drop onto the coating substrate by means of the hypodermic syringe. The substrate consisted of a filter paper strip fed into the sample compartment of the spectrofluorimeter with the help of a Teflon-coated worm drive mechanism. Prior to depositing the samples were dried by passing the filter paper strip through a flame-dried chamber equipped with an infrared lamp. The drying time could be controlled by adjusting the paper roll speed with the handwheels. The area required for analysis depended upon the optimal drying time, which was chosen in accordance to the highest signal-to-background ratio obtained for each compound. Most tested phosphors showed the highest ratios when they remained for two minutes in the drying chamber, allowing us further I R measurements per minute. The life of most series of measurements of 16 to 22 theoretical samples were found to be less than 10. The last were at the sample level for pyrene, phenanthrene and chrysene dissolved in a solution of nitrobenzene (1/1, v/v) containing 0.1 M HgCl_2 , and for BBA dissolved in an aqueous solution of NaOH (0.1 M/0.1 M). Later, the system was modified by Yen-hsue and Winderbaum [31]. The new drying unit consisted of an L-shaped stainless tube heated with heating tape, stopped with asbestos, and placed directly above the sample compartment of the sodium-fluorescein spectrofluorimeter. A new filter paper guide, which was made from a cylindrical stainless block, was mounted inside the sample compartment by means of the supporting covers. A mechanism stopped and an analog output phosphoroscope were incorporated for time resolution. The frequency of the mechanical chopper for the excitation light was 100 Hz, the gate period of the analog output was set at 4 ns and the delay interval between the excitation pulse and the detection was set at 0.5 ns. The analog output system allowed better control of time resolution than did the recording device. All at about 10 and 100 in the sample level were obtained for pyrene and phenanthrene in ethanol/0.1 M HgCl_2 , and for BBA in 0.1 M NaOH - 10 Hz. Although considerable reduction of analysis time with no loss in sensitivity was also achieved with this system, the samples were still manually applied with a hypodermic syringe or the

moving ECRist paper. For each measurement, the filter paper was swapped and the phosphor spot was aligned with the excitation beam. The excitation ECR selection was then obtained by rotating the cylindrical filter paper guide into the sample compartment of the instrument.

This study reviews the development of a new experimental system for the estimation of ECRF. The major steps resulting in the previously described system [4,19] have been eliminated. Simple and heavy ion selection are continuously sprayed onto moving ECRist paper strips by means of solenoids. A ion sample holder was designed and adapted to the cell compartment of a Berkeley-Lane L3 spectrometer/monitor coupled to a Model 440 data station. Known to twenty measurements per channel are easily taken, reducing the sampling time usually required for ECRF analysis. Resolvable L20 and L25 in three particularly required [4,19] were obtained, showing that the proposed system is a convenient approach towards the estimation of ECRF.

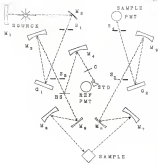
Experimental

Instrumentation

The ECR specter and intensity measurements were performed with a Berkeley-Lane L3 Continuous spectrometer/monitor (Berkeley-Lane Form 40, CT) introduced to a Model 440/400 data station. A block diagram of the detection unit is depicted in Figure 3-1 [19]. This spectrometer measures the fluorescence or phosphorescence of luminescent samples within a continuous scan over the selected wavelength range (200-600 nm) of interest or at predetermined points within the range. The source is a pulsed neon flash tube that is of high intensity short duration and covers the ultraviolet visible region. Energy from the source is collimated and defocused onto the entrance slit of the detection monochromator (150 lines per cm grating). All wavelengths of excitation energy are eliminated by the grating, and a prism is placed in the beam splitter. In the beam splitter a small fraction of the energy is directed through a compensator onto the reference cell containing a solution of Rhodamine 6G, dye. The compensator compensates for the

Figure 7-1. Schematic diagram of a Perkin Elmer LS 1 Spectrofluorometer

M. mirror
 E. slit
 R. rotating
 OS. beam splitter
 C. component
 REF. PMT. reference photomultiplier tube
 SAMPLE PMT. sample photomultiplier tube
 STD. standard



varying reflectivity of the beam splitter. The detection dye absorbs energy in the 328-330 nm range and fluoresces at about 600 nm with excellent quantum efficiency. This fluorescence is directed into the reference photomultiplier detector (RD). The output portion of the excitation beam is focused by the mirrors onto the entrance slit of the emission monochromator (440 lines per cm grating). A narrow band of energy is diffracted by the grating, through the exit slit and onto the sample PD. The outputs of both the sample and reference paths are processed by ratio-sensing electronics to produce an output that is proportional to the ratio of the signal from the sample that has been corrected for variations in the intensity of the source with respect to wavelength. The selected intensity and corresponding excitation and emission wavelengths selected by the monochromators are indicated digitally and the corresponding outputs can be read from a printer (digital) and recorder or computer (analog). Time discrimination was used to distinguish between fluorescence and phosphorescence emission: a pulse delay time of 0.50 ns and a gate time for collection of data of 1.0 ns were used for all phosphorescence measurements. The excitation and emission slits were set at 1 and 10 nm, respectively. The original angle holder of the instrument was replaced by a laboratory-constructed film paper guide (Figure 1-10). Two rolls on the base of the film paper guide allowed the vertical block to slide back and forth which provided a coarse for the film paper strip to run smoothly and continuously through the sample compartment of the detection unit. The position of the irradiated area on the film paper strip for maximum RRF signal needs to be optimized by sliding the vertical block back and forth. After obtaining the optimum position, the vertical block could be firmly fastened by means of a set of screws to maintain in a constant position during all experiments.

The different ways of spraying solutions on the film paper strip were tested for best results. In the original design which can be seen in Figure 1-3, a conventional streak absorber unit was employed to spray the analysis solution previously mixed with the heavy-metal solution.

Figure 3.8 Schematic diagram of a dilute paper guide used for a continuous roll substrate from temperature/pressure mapping system. (a) front view of the dilute paper guide having the mentioned layout of the registration marks (b) back view of the dilute paper guide having the standard four continuous dilute (c) bottom view of the dilute paper guide

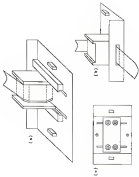


Figure 3-6

Three views of an instrument sampling system for continuous solid inclusion from atmospheric phosphorus samples employing an aerosol absorption technique as a reduction/oxidation device.

(1) Prior to pump roll. (2) Aerosol sampling (mid/roll). (3) Drying chamber. (4) Oxidation/absorption. (5) Dried/acid sample components. (6) Spectrophotometer readout. (7/8/9)



The drying unit consisted of an aluminum chamber equipped with an infrared lamp and a thermometer to monitor the temperature ($<10^{\circ}\text{C}$). While in operation, sides of the drying chamber permitted two parallel stainless rods to pass through, leaving a space for the filter paper. A groove 3 mm wide and 4 mm deep in each rod held the position of the filter paper constant with respect to the sublimator. Four stainless posts retained the rods and the drying unit above the level of the spectrophotometer. Both rods entered the detection unit, and a Tachistron Industries continuous filter (Tachistron Instruments Corp., Tachistron, NY) was used to pull the filter paper through the sample compartment. Stainless rollers (shown in appropriate positions from Figure 2-1) helped the filter paper to run smoothly through the system.

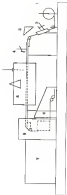
The second approach is a modification of the original design and utilized two concentric sublimators to separately spray the heavy area and the analyte solutions onto the moving filter paper strip. A schematic diagram of the design can be seen in Figure 2-4. Prior to deposition of analyte solutions on the substrates, the heavy area solutions were dried onto the filter paper strips by means of an infrared lamp. The relative positions of heavy area and analyte sublimators were optimized in such a way that the analyte solutions were sprayed on the same area of filter paper previously sprayed with heavy-area solutions.

Reagents

Pure *p*-nitrobenzoic acid and succinic (Fluka Chem. Co.; Technicon, NY), pyrene (Oxy Chemical Corp.; 99.1-99.9- α -chloranthenes (2,3,5,8-BA), phenanthrene and fluoranthene (Molecular Chemical Co. Richmond, NY) were reagent grade and used as received. Thallium chloride (TlCl_3) was obtained from Mallinckrodt (St. Louis, MO) and sodium lauryl sulfate (purify of 95%) was purchased from Sigma Chemical Co. (St. Louis, MO). Sodium lauryl sulfate was prepared in our laboratory. Ten Fluoradene Silver chloride (AgCl) was purchased from Sigma Chemical Laboratories, Inc. (St. Louis, MO), sodium iodide was obtained from Fisher Scientific Co. (Fair Lawn, NJ), thallium (I) acetate (TlAc) was from

Figure 3-4

This view of an example coding system for sentence with subjects and subjects pluralization analysis applying the example sentence in subject position shows: (1) First step in: (2) base form subject, (3) inflect (imp), (4) analyze subject, (5) begin subject, (6) plural make compound, (7) present tense, (8) subject tense



aluminum chloride (AlCl_3), aluminum metal (Al), and lead (Pb) acetate (PbAc) from Allied Chemical (Nutley, NJ). Acetic anhydride (Fluka Manufacturing Co., Lake Alfred, FL) and "municipal" deionomized water, Barnard Systems Corp., (Boston, MA), were used to prepare all solutions. No. 100-B and No. 1-a filter paper (Whatman and Whatman, Inc., Waco, TX) were obtained as 12.5 cm wide and 25 cm long filter paper rolls to be used as substrates.

Experiments

Automated spray deposition on static deposition substrates.

Preparation of TMS. TMS was prepared by a procedure similar to Humphrey-John, et al. [13]. Aqueous solutions of 0.01 M acetic anhydride (AcAc) and 0.01 M TiCl_4 were prepared. A 250 ml. aliquot of the AcAc solution was mixed with 500 ml. of TiCl_4 solvent. The mixture was stirred and gently warmed for approximately 2 h. removed from the heat and subsequent cooling of the mixture to room temperature initiated formation of the white precipitate, TMS. The precipitate was collected after 24 h., isolated by gravity filtration washed with deionomized water and allowed to air dry for 24 h. TMS was then reprecipitated from water until the melting point of TMS became constant at 177°C . a 40 percent yield of colorless crystalline product was obtained.

Preparation of Solutions. A mixture of acetylacetone 10:20 v/v was used to prepare 0.001 M TMS and 0.1 M TiCl_4 solutions. 1 M AcAc and 0.1 M TiCl_4 solutions were prepared in acetylacetone 10:50 v/v. The acetylacetone solutions were then used as solvents for standard solutions of PAA, acetate, and pyrene.

Automated Deposition. The initial volume of the sprayed solutions was 1 ml. Flow rates were adjusted to deliver 4 μl of solution per cm^2 of filter paper (0.5 cm \times 0.5 cm substrate spots). After a section of filter paper of the desired length had been sprayed, the solution flow was stopped and the sprayed section was drawn into the drying chamber and remained for approximately 2 min. The RTF signal was then measured. After each measurement, the acetylacetone slit was raised, the filter paper was moved and a new spot of the sprayed section was passed in front of the acetylacetone slit. Since the length of the irradiated spot was

approximately 1 cm. or less) due to take several measurements for each surface of filter paper sprayed. All the measurements were performed in the presence of dry nitrogen at the maximum excitation and selective wavelengths of each analyzer. The background signal was obtained by measuring the RFP intensity of the filter paper sprayed with the heavy zinc solution at the respective maximum excitation and emission wavelengths of each analyzer.

Automatic System Developing For Continuous Fluorescence

Preparation of Solutions A mixture of ethanol/water 50:50 v/v was used to prepare 1 M NaCl, 0.5 M HClO₄ and 0.1 M TlCl₃ solutions, all analyzer solutions were prepared in absolute ethanol by serial dilution of 100 mg/ml stock solutions.

Experimental Procedure The heavy zinc and analyzer solutions were simultaneously sprayed onto the moving filter paper strip. In both cases the initial volume was 1 μ l, and the flow rates of both solutions were adjusted to deliver 5 μ l of solution per cm of filter paper strip (10 cm/min filter paper speed). The same measurement procedure as the one previously described for the one analyzer system was then employed through all experiments.

Results and Discussion

The performance of the continuous coupling system employing an etched tungsten cathode was evaluated by testing three toxic phosphorus compounds: cyanide, thallium, and arsenic. Initially 1 M NaCl, 0.1 M AgCl₃ and 0.1 M TlCl₃ were tested as heavy zinc solutions. However clogging of the cathode was observed which affected the reproducibility of the measurements. This problem was a result of the high concentrations of the heavy zinc salts utilized. A solution of the heavy zinc salts was possible but was inconsistent above the best RFP measurements with these procedures are obtained at these higher concentrations [4-6].

In future studies [11-13] we demonstrated that TlCl₃ is a suitable heavy zinc reagent for RFP analysis of polychlorinated biphenyls even

when it is present at low concentrations of 0.1-0.8 mM. As a result 0.008 M TLA was employed as a heavy-ion scatterer instead of the former modified cells. Table 3.1 lists the analytical figures of merit (AFM) of the three compounds studied. The calibration curves were linear over 3 decades, and the slopes of the log-log calibration plots were all close to unity, with excellent correlation coefficients. The absolute detection limits were calculated under the assumption that the amount of spray being used was 1 μ l of solution per cm of filter paper, which corresponded to the length of the irradiated area in the sample compartment. Possible surface losses were not taken into consideration, the assumption being that the complete volume had been deposited onto the filter paper. LODs in the sample range were obtained for Mn, and pyrene, and a value approximately 60 times lower was found for captopril. The precision of the method for all the analytes was less than 7% which was statistically the same as the precision of the background correction. Our results were comparable to those previously obtained in the literature and obtained by manual procedures commonly used in GMP analysis [4, 6, 71, 72]. However, such shorter analysis times were achieved when the proposed sample holder and the waste absorption substrate were used to perform the measurements. Calibration curves resulting from six measurements each of six replicates of different analyte concentrations were obtained in less than 2 hr of analysis time. Measurement of the precision for the method, which is usually a long and tedious experiment, was accomplished in less than 30 min. By a reduction in drying time, further analysis could be performed, but no experiments were done in order to optimize this parameter.

An important disadvantage of the proposed system, though, was the clogging of the nebulizer by high concentrations of heavy ions when in GMP analysis maximum signal enhancement was usually obtained with particular concentrations ranging from 0.1-2 M [4, 15]. A convenient automatic system, therefore, should possess the capability to work with heavy-ion solutions at their optimum concentration ranges to obtain the best sensitivity for the whole variety of phosphors. As a conclusion

means to achieve the required versatility - a chemically resistant liner for the deposition of heavy atom solutions was tested. The more homogeneous results obtained by the chemically resistant liner on the filter paper strips encouraged us to utilize a similar one to spray the analyte solutions, replacing the usual absorption cellliner employed in the original system. An infrared lamp placed between the two substrates avoided the trouble of removing the analyte solutions or wet substrates, restricting the possible increase of analyte adsorption to the edges of filter paper strips. The versatility of the modified system was then verified by testing those heavy atom solutions (Ba, Bi, Pb, Sb, Sn, Tl, Zn) which are commonly used in XRF analysis to determine a large variety of elements at the nanogram level [5,16,17]. Table 1.1 lists the XRF obtained with these heavy atom standards on six well known phosphorus compounds including Fe, Mn, cobalt, copper, Li, B, V, Nb, Ta, Mo, W, Ni, Zn, Cd, Pb, Bi, Sb, Sn, Tl, Zn. The XRF were calculated considering that 5 μ l. of solution were sprayed per cm of filter paper, which corresponded to the length of the irradiated area in the sample compartment. Sample's volume losses were not taken into consideration, assuming that the sprayed volume had been deposited onto the filter paper. These values were in the nanogram level, which agrees favorably with those reported in the literature [5,16,17]. With the exception of Li, B, V, Nb, Ta, Mo, W, Ni, Zn, and Fluorine...all the analytes showed calibration curves with \log over 2 orders of magnitude. In all cases, the slopes of the log-log calibration plots were close to unity with excellent correlation coefficients. The precision of the method ranged from 1.2 to 30%, which is within the range usually observed for XRF analysis [5,16,17].

Conclusions

This study showed that the proposed system is a reasonable advance towards the automation of XRF. The manual steps involving the previously reported automated systems [5,17] were eliminated. In these systems [5,17], the solutions were sprayed onto the moving filter paper by means of a syringe-like syringe and the optical path was for various XRF signals

Table 3.1: Analytical diagrams of multi-physics for Boltzmann Transport Phenomena (which are presented by simplifying System Simplifying Two Subdomains as Energy Atom and Analytic Interacting System)

Component Evaluation	Physics	Energy	λ_{eff}	λ_{eff}	Unit	Log Log	Log Log	Correlation	Log	Result (H)
Energy	Energy	Atom	240	450	2.500	0.16	0.000	0.000	1.45	1.4
Energy	Energy	Atom	240	450	2.500	1.00	0.000	0.000	0.16	0.0
Energy	Energy	Atom	240	450	2.500	0.16	0.000	0.000	0.00	0.0
Energy	Energy	Atom	240	450	2.500	1.00	0.000	0.000	0.16	0.0
Energy	Energy	Atom	240	450	2.500	0.16	0.000	0.000	0.00	0.0

a. Model depends upon simplifying two via measurements of each analysis simplification.

b. Limit of diffusion calculated by $\lambda_{\text{eff}}/\lambda_{\text{eff}}$. Where λ_{eff} is the physical diffusion of 31 blocks, and λ_{eff} is the slope of the analytical intercalated curve plotted on linear space correlation.

c. Precision for the device was obtained by the following formula:

$$\text{Error} = \frac{\sqrt{\frac{1}{N} \sum_{i=1}^N (x_i - \bar{x})^2}}{\bar{x}}$$

where λ_{eff} is the diffusion of 31 the analysis and other respective blocks were utilized to determine the standard deviation of each a block intensity λ_{eff} standard deviation of block size boundary and λ_{eff} average size analysis, DTP density

had to be checked for each sample by clipping the sample spot on the substrate with the excitation beam of the spectrofluorometer. Although completion of 1 measurement per minute was reported [31], the optimization step for maximum EFT signal was tedious and required a certain degree of experimenter's expertise.

The new sample holder employed in our system allowed the strip of filter paper to run at a constant position through the sample compartment of the spectrofluorometer. The optimum position for maximum EFT intensity was easily obtained by sliding the vertical block of the sample holder on rails with the exposed part of filter paper and the irradiated area of substrate. The vertical block position and the relative positions of both substrates were then kept constant through all experiments, avoiding the need of optimization for each measurement. Almost as many measurements were easily taken in less than one minute and the polar anisotropy curves were obtained in approximately one hour of analysis time. Clipping problems with heavy-ion solutions were solved by employing the appropriate substrate, providing the measured system with the versatility needed to perform rapid EFT analysis. Compared to 150 and 120 as shown previously reported by us and [44] or somewhat [45-51] procedures were obtained with shorter analysis times, showing that the proposed system is a successful approach to develop the full potential of EFT as an analytical technique for routine analysis. In addition, the successful performance of the two substrate system suggested the possibility of using EFT as a detection technique for HPLC. The role of the spectroscopic column can be easily adapted to the analysis substrate by means of a scanning rate. The use of a different substrate for heavy-ion depositions and the fact that a large portion of these substrates are previously commercialized to deposit the analysis substrates provides compatibility problems with the whole phase employed for separation.

CHAPTER 4

FLUORIMETRIC AND THERMAL ANALYSIS DETECTION FOR HIGH PERFORMANCE LIQUID CHROMATOGRAPHY

Introduction

In some cases, the selectivity of HPLC allows the qualitative and quantitative analysis of multicomponent mixtures without previous separation. When the desired compound is the phosphorescent phosphor of the mixture, the excitation and/or emission spectrum of the sample can be directly used for detection purposes [14-11]. Van Dorsselaere and Martelien [14] employed carbon tetrachloride as a solid substrate to determine the concentration of BMD in vitamin tablets. The tablets investigated also contained vitamin B_2 , B_6 , B_{12} , and B_{15} , folic acid, pantothenic acid, cholecalciferol, inositol, choline, inositol, and lysine. The method was so specific for BMD that the tablet extract exhibited ETP excitation and emission spectra identical to those of pure BMD samples. Smith and Winfordham [11] reported a simple HPLC procedure to analyze thiophylline and related compounds such as aminophylline, xanthine, and aminophylline in pharmaceutical preparations with no previous separation. The selectivity was achieved because no compound other than the active ingredient being analyzed presented ETP under the experimental conditions employed.

When the sample contains several compounds with phosphorescence maxima of comparable intensity, the similarity matrix overlapping of these phosphorescence bands usually interferes in the differentiated process of single compounds. Several alternatives have been proposed to overcome this problem [14-16, 11]. Relative optimal heavy atom quenching (RHAQ) has been employed for the analysis of organic compounds in solution without previous separation. Van Hest and Boeyens [17] were able to determine benz[a]pyrene at the nanogram level in a

synthetic mixtures containing acetone, carbonic diethoxycarbamate and fluoranthene in about 100-fold excess. The high selectivity was the result of using a properly selected absorptive substance (East Hill acetate) in combination with a convenient set of measurement wavelengths (190-250nm) which strongly eliminated spectral interferences from other components of the mixture. Jacoby-Atjage et al. [75] took advantage of the differences in RFP inducing interferences between phosphoric and carbonic to achieve better sensitivity with RSPFP. A study of the RFP characteristics of various pesticides showed the possibility of determining naphthalenemethoxycarbamate and 1-indolmethoxycarbamate in the presence of 1,5-dithionaphthalene, and 1- and 2-naphthol acid without previous separation. When FAL filter paper, acetone and the acetic acid/carbonic anhydride wavelength of naphthalenemethoxycarbamate were used in the determination, all the other compounds showed very low RFP signal formation. Similar results were observed with 1,5-dimethoxycarbamate in mixtures spotted on the same kind of filter paper but in the presence of carbonic anhydride. The single determination of the other substances, though, was not possible due to interferences from other compounds in the mixture.

Spectral interferences can be considerably reduced by synchronous phosphorescence. Yu-Hsiu and Huang [76] were the first to introduce the synchronous technique, analogous to phosphorescence analysis in solid solutions. A synchronous phosphorescence spectrum is obtained by scanning both the emission (λ) and excitation (λ_0) wavelengths simultaneously while keeping the spectral interval $\Delta\lambda = \lambda - \lambda_0$ constant. If $\Delta\lambda$ is chosen to be equal or larger than the wavelength separation between the lowest singlet and lowest triplet states (λ_{ST}) of a given compound, a synchronous phosphorescence signal of that compound will be observed. On the other hand, the synchronous signals of those compounds deviated with λ_{ST} values larger than the experimental $\Delta\lambda$ values will not be observed. In addition to the improvement in selectivity provided by λ_{ST} , synchronous phosphorescence spectra have shown narrower bands than

conventional species. Additionally even more the possible interferences due to spectral overlapping. The technique was employed to facilitate the differentiation between ethionazepines (ENs) isomers 1,2,3,4-ENs and 1,3,5,4-ENs, which is made difficult by spectral overlapping in conventional GC/MS. It was possible to detect 0.1 ng of 1,2,3,4-ENs in a binary mixture containing 50-fold in excess of 1,3,5,4-ENs, showing the potential sensitivity of synchronous scanning in GC/MS analysis. Its use in routine analysis, however, strongly depends on optimizing the scanning procedure of all values for compounds of interest. Future work needs to be done in this area to extend its application to the wide variety of compounds analyzed.

Although the alternatives described above improved the sensitivity of GC/MS in specific situations, separation prior to MS detection is usually convenient when dealing with complex mixtures. Several authors have proposed paper and thin-layer chromatography (TLC) as separation techniques for GC/MS detection [36,37]. Ford and Hershman [38] utilized silica gel chromatograms as solid substrates for the MS analysis of pesticide residues. Twine and Macle [39] employed paper chromatography (PC) to separate synthetic steroids of 19-n-pregnenolone and some of its derivatives. The separations were performed on filter paper strips which were driven from the sample compartment of the spectrophotometer by means of a laboratory constructed paper chromatography assembly. The unique possibility of complete analysis of complex mixtures using the same substrate from PC-MS or TLC-MS combinations have relatively simple and useful tools for analytical purposes.

GC/MS has also been associated with HPLC [4,70]. Filter paper discs were utilized by de Haas and Wiersma [4] to quantitatively determine benz[a]pyrene and benz[a]pyrene in anal. liquid samples. Ford and Hershman [38] used silica chromatograms to identify benz[a]pyrene and phenanthrene in whole cell samples. In both cases [4,70] the HPLC fractions were usually collected and spotted onto the substrates for GC/MS detection.

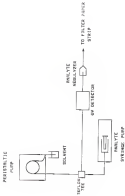
In this study, the two sublinear system described in Chapter 3 for the estimation of ISTD is optimized as a selective detector for HPLC as a preliminary step for the use of the automated device in a flowing system such as HPLC. Flow injection analysis (FIA) was employed as a continuous sample introduction approach. These well known phosphorescent compounds were successfully tested, showing the feasibility of using the automated system for a continuous mode. The performance of the ISTD system for HPLC detection was then evaluated by comparing the chromatographic parameters and the APM of flow responses obtained with the automated system to those obtained by UV absorbance detection. The versatility and selectivity of the ISTD detector was demonstrated by identifying overlapped compounds eluted from the ISTD chromatograms as free state ITP species chromatograms.

Flow Injection Analysis for Continuous Sample Introduction in ISTD: Experimental

Instrumentation Figure 4-1 shows a schematic block diagram of the FIA system used as a continuous sample introduction device. A syringe peristaltic pump (Rainin Instrument Co., Whittier, CA) and a novel (N) syringe pump (Iga Instruments Inc., Woburn, MA) were used to respectively mix the solvent and the analyte solution at different concentrations ratios. A Teflon line (Rainin Instrument Co., Whittier, MA) was employed as mixing chamber and Teflon tubing (0.1 mm i.d.) was used to make all connections. A Teflon needle (N) UV detector (IDA) was placed prior to the analyte solution peristaltic controlling of the concentration of solutions injected into the mixing filter paper. A pulse delay time of 0.00 ms and a gain time for evaluation of data of 0.0 ms were used to perform all phosphorescence measurements under a flow of dry nitrogen. The excitation and emitting slits were set to 1 nm and 10 nm, respectively.

Reagents All the chemicals were analytical reagent grade and used as received. Polysilyl-substituted urea was purchased from Eastern Organic Co. (Horseshoe, NY) and pyrene, phenanthrene and choline (1) acetate (CTOAC) were obtained from Aldrich Chemical Co. (Milwaukee, WI).

Figure 4-3. FGA spectra used as a quantitative sample characterization device for measured polymer analysis.



Absolute ethanol (Fisher Hareline 40 : Lake Arrow, FL) and "concentrated" hydrochloric acid (Fisher Special Reagent, Boston, MA) were used as solvents to prepare the solutions. 1 x 10⁻³ M and 1 x 10⁻⁴ M films (Gardner and Schmitt, Toronto, ON) was obtained as a 1 x 1 cm slide or as a long film paper (10 x 10 cm) and utilized as a substrate.

Procedure - A 0.1 M HCl solution in ethanol/water (50:50 v/v) was employed as a carry-over solvent and continuously sprayed onto the moving film paper at a flow rate adjusted to deliver approximately 10 μ L of solution per cm² of substrate (20 cm/min film paper speed).

By keeping the flow rate of ethanol (50:50 v/v) constant and varying the flow rate of analyte solutions, it was possible to obtain a set of concentrations ranging from 1.5 μ L/mL to 161 μ L/mL. Since no ions were introduced in calculating an approximately constant volume of solution

sprayed to the substrate (20 μ L/cm² - 100 μ L/mL and 160 μ L/mL, each analyte solution was employed for the lower (5-25 (5 μ L/mL) and upper part of the calibration curve, respectively. Table 4-1 lists the different syringe pump flow rates used with the FIA system, the total flow rate, the analyte concentration of the sprayed solutions, and the mass of analyte deposited per cm² of film paper.

All the measurements were performed in a continuous mode with the use of a kinetic program which permitted plotting the phosphorescence intensity as a function of sampling time. A fixed sampling time of 80 μ s and a data interval of 0.1 μ s were employed to obtain 160 points per "spectrum". While the desired section of sprayed film paper was passing through the sample compartment of the spectrophotometer, the excitation slit was opened and the UV solution to the maximum excitation and emission wavelengths of the respective analyte was registered. Considering the film paper speed, 80 μ s of sampling time allowed the registering the phosphorescence intensity of 16 cm of sprayed substrate. Since the length of irradiated area was approximately 1 cm, the equivalent of 16 different samples were measured during that period of time. The

Table 4.1. Analyte Concentrations Deposited onto the Moving Filter Paper With a Flow Injection Analysis System as a Continuous Sampling Introduction Device for Solid Substrate Film Deposition Phosphorimetry.

Flow ^a ($\mu\text{L}/\text{min}$)	Flow ^b ($\mu\text{L}/\text{min}$)	v_p ^c ($\mu\text{g}/\text{cm}^2$)	Mass of Analyte ^d ($\mu\text{g}/\text{cm}^2$)
1.4×10^{-3}	9.69×10^{-2}	3.5	0.023
1.0×10^{-3}	3.60×10^{-2}	1.0	0.006
1.34×10^{-3}	1.10×10^{-1}	12.4	0.128
1.34×10^{-3}	1.34×10^{-1}	18.3	0.193
9.4×10^{-4}	1.08×10^{-1}	16.0	0.168
1.00×10^{-3}	1.17×10^{-1}	17.8	0.182
1.34×10^{-3}	1.34×10^{-1}	141.0	1.177

^aFlow = flow rate of water-analyte solutions from the syringe pump.

^bFlow = total flow rate of analyte solutions. Calculated by adding the solvent flow rate to Flow^a.

^cConcentration of analyte solutions sprayed on the substrate.

^dMass of analyte deposited per cm^2 of filter paper. Calculated by the following equation: $(\text{Flow}/v_p) \times v_p$, where $v = 18.3 \text{ cm}^2/\text{min}$ is the area of substrate sprayed per min when film deposition was speed of the moving paper (11 cm/min) and the width of the sprayed path (0.5 cm).

^eTotal solution concentration: 500 $\mu\text{L}/\text{mL}$ (water) + 500 $\mu\text{L}/\text{mL}$ used for the three four flow rates.

of the filter paper soaked with heavy metal and organic solutions at the maximum excitation and emission wavelengths of each analyte. No significant differences in the background signal was observed for the different flow rates used for calibration curves.

Results and Discussion

The performance of the continuous sampling system was evaluated by testing three well known phosphors which have been extensively studied by IAEA [4]. The choice of these phosphors and systems as probe compounds allowed comparison between the performance of the system operated in a continuous mode and that obtained with the procedure described in Chapter 1, when the filter paper strip was stopped for signal detection. 2,2,6-Tri-*n*-butyl-1,3,5-triazine was selected as a heavy metal phosphor, being particularly efficient in the enhancement of the phosphorescence emissions of polycyclic aromatic hydrocarbons (PAH) such as pyrene and phenanthrene [44].

Table 5-1 lists the LODs obtained with the FIA system in a continuous sample introduction scheme. Each phosphorescent intensity plotted in the calibration curves is the average of 12 replicates taken from the diagram at every 3 s between 60 s and 180 s of sampling time. The limits of analyte sensitivity for the phosphorescent signal were calculated from the values listed in Table 5-1 ($\mu\text{g}/\text{m}^3$) considering an injected area of 2.5 cm^2 . The limits of detection were obtained from the equation $s_L = 3s_0/m$ where s_0 is the standard deviation of the blank during the sampling time (s=2) and m is the slope of the analytical calibration curve plotted as linear-linear coordination [45].

The precision of the method was determined from the formula $P = (s_{\text{std}}/x) \times 100$ where s_{std} is the standard deviation of 12 measurements of the phosphorescent intensity of 100 μg of analyte-blank, s_0 is the standard deviation of the blank and x is the average net analyte signal.

With the exception of pyrene, the other analytes showed in calibration curves with linear dynamic ranges of approximately 2 orders of magnitude. In all cases, the slopes of the log-log calibration plots were close to unity with excellent correlation coefficients. The LOD was in

Table 4-1 Analytical Figures of Merit, Discontinuous Flow Injection Analysis System in a Continuous Sampling Introduction Section for Solid Substrates from Temperature-Dependent Analysis

Compound	I_0 (mV)	I_{∞} (mV)	$\log I_0$ (mV)	$\log I_{\infty}$ (mV)	Correlation (r^2)	\log^2 (mV)	Percentage of Rejection (%)
Urea	334	420	11.5	10.6	0.994	1.27	12.44
Formamide	334	503	15.5	6.45	0.994	2.36	12.45
Glycine	343	575	15.5	1.46	0.993	4.39	12.47

r^2_{100} = Linear Dynamic Range

r^2_{100} = Limit of Detection

the negative slope which compares favorably with the ones reported in the literature [5] and with those obtained by stripping the filter paper at the measurement time (see Chapter 3). The precision of the method, however, was a little poorer than expected. The use of FIA as a calibration-transfer technique offered no advantage for a highly reproducible mixing of components whose concentrations were continuously manipulated and measured [14]. The RSD obtained, though, was higher than those obtained in Chapter 3 when a batch procedure was employed to prepare the solutions sprayed onto the substrates ($2.2 - 3.0\%$). Several reasons can be given for the higher variances observed. First, in the actual procedure the measurements were taken in a continuous mode; the noise caused by the action of the pump and possible concentration fluctuations induced by the peristaltic flow could explain, to some extent, the observed results. Due to limitations of the peristaltic pump employed, smaller volumes than $10\ \mu\text{L}$ per cm of filter paper could not be sprayed. This is approximately twice the volume utilized in the procedure described in Chapter 3. The deposition of large volumes ($60\ \mu\text{L}$) on filter paper can cause the migration of the analyte to the edges of the substrates [5,10,11,14]. Hence the migration is not uniform and the streffed area on the substrate was kept constant through all measurements. The spreading of analyte on a larger area of substrates could be responsible also for the higher variances observed in RSD signals. Finally, the larger values of signal sprayed on the filter paper and the fact that the spraying time exceeded the one as the one used in Chapter 3, could lead to physical quenching by solution of analyte signals deteriorating the precision of the method.

The higher RSD observed indicates the possibility that the precision of the method is mainly related to phenomena occurring at the surface of the substrate instead of improvements relevant to batch procedures. The use of a different peristaltic pump which would allow the deposition of convenient volumes of solution ($< 5\ \mu\text{L}$) on the filter paper strip could probably be more suitable for FIA-RSD analysis. However, the FIA-RSD

system employed in a continuous mode produced reproducible LOD and LOQ to the ones obtained in Chapter 3, showing the feasibility of using the HPLC automated system as a selective detector for HPLC analysis.

Utilization of the Two-Subchannel Automatic System as a Continuous HPLC Detector for HPLC Analysis

Instrumentation. The HPLC system consisted of an Alcon model 111B pump used with a Rheodyne valve and a 10 μ L sample loop. The Alcon column was 15 cm long, 4.6 mm I.D., and filled with atmosphere 995 (low porosity diameter). The UV detector was an Alcon model 103 with a cell volume of 2 μ L, response time constant of 1 s and fixed wavelength at 226 nm. The two-subchannel system for HPLC detection was employed without previous modifications. The eluent from the chromatographic column was sprayed onto the wetting filter paper strip by connecting, with a Teflon tube (0.15 mm I.D.), the outlet of the UV detector cell to the analyte inlet of the automatic system. The Teflon tube was kept as short as possible (20 cm) to minimize band broadening. All the HPLC measurements were performed under a flow of dry nitrogen with a delay time of 0.20 ms and a gate time for collection of data of 0.2 ms. The resolution and the detection limits were set to 20 ms and 1 ms, respectively.

Reagents. All chemicals were analytical reagent grade and were used as received. Octadecyl was purchased from Fluka. Toluene, *p*-xylene, hexane(*n*-hexane), fluoranthene, phenanthrene and chrysene (11 sources (TICs)) were obtained from Aldrich Chemical Co. HPLC grade methanol (Fisher Scientific Co.) and "nanopure" deionitized water (Nanopure System Inc.) were used throughout. 4.6 x 10³-A filter paper (Schleicher and Schuell) was obtained as a 1.5 cm wide x 25 cm long filter paper roll, and was utilized as a substrate. Methanol/water solution of different column ratios were employed as solvents to prepare 100 μ g/L stock solutions of acenaphthene and phenanthrene (50:50 v/v), and pyrene and fluoranthene (30:70 v/v). The same mass of hexa(*n*-pyrene) was dissolved in pure methanol. A 0.1 M solution of TICs in methanol/water 50:50 v/v was employed as a binary-ion solution.

Experiment. All the RFP measurements were performed in a continuous mode with the use of a kinetic program which permitted plotting the phosphorescent intensity as a function of time. While the desired portion of Elliot paper was passing through the sample compartment of the spectrophluorometer, the excitation slit was opened and the RFP induced in the selected emission and emission wavelengths was registered. The total sampling time was chosen according to the separation time in the chromatographic column and a delay (interval) of 4.2 s was kept constant through all the experiments. For all the RFPs, a sampling time of 800 s was employed to obtain 4000 points per chromatogram. The whole photo-decay process introduced a delay time of 150 s. This delay time in the RFP chromatogram corresponded to the time spent by the analyte in the solution to "travel" from the solution to the excitation slit of the spectrophluorometer. Hence the time spent for the effluent to go from the UV detector to the analyte cell was negligible for all the flow rates tested, the same delay time was observed for all the experiments. The retention times in the RFP chromatograms were then compared with respect to the observed values (10) (4).

Results and Discussion

Five well-known phosphorescent compounds: carbazole, phenanthrene, pyrene, benz[a]pyrene (B[a]P), and fluoranthene were selected to compare the UV and the RFP system for RFP detection. All of them strongly absorbed at 254 nm at which the UV measurements were performed. The 3,3',3'-TMAA solution, chosen as a heavy-ion perturbation, was shown to be particularly efficient in the signal enhancement of most of the probe analytes (4, 16).

Figure 4-1 shows a RFP chromatogram along with the corresponding classical UV chromatogram of a mixture containing carbazole, phenanthrene, pyrene, and B[a]P. In order to simplify the measurement procedure, only one mode of detection wavelength was employed. The measurement wavelengths selected took into consideration the relative phosphorescent intensity of the studied compounds. When necessary, the chosen wavelength

Figure 1.1

Figure 1.1 is a diagram illustrating the relationship between the concepts of "Identity" and "Difference". The diagram consists of two overlapping circles. The left circle is labeled "Identity" and the right circle is labeled "Difference". The overlapping area in the center is labeled "Intersection". The text "Figure 1.1" is located at the top left of the diagram.

pair was not closer to the wavelength for maximum RF signal of the visible phosphor. The wavelength and chromatographic parameters are listed in Table 4-3.

Chromatographic Band Broadening. The peak efficiencies were obtained assuming Gaussian peaks and are listed in Table 4-3. The low efficiency obtained for naphthalene ($R_{\text{eff}} = 125$, $R_{\text{the}} = 150$) was not surprising. Naphthalene, whose other name is dicarbazole, is an arine containing basic compound. The -NH amino group of the pyridic ring has a high affinity for surface silanols of the silica stationary phase. This affinity induces a peak tailing and low efficiency. The relatively low efficiency observed for phenanthrene ($R_{\text{eff}} = 1250$, $R_{\text{the}} = 1350$) may be due to arine volume band broadening effects apart from the dispersion. In paper we note that the chromatographic system was not optimized for maximum efficiency. However, it is interesting to estimate the band broadening induced by the HRP detector. A 114 efficiency loss was observed in comparing the RF absorption in the HRP column (Table 4-3). The band broadening produced by the measuring tubing, catheter and moving paper strip can be roughly quantified through variance calculation using the equation $\sigma^2 = \sigma_{\text{p}}^2 W$. Defining σ_{meas} and σ_{in} from HRP and the RF absorption chromatograms, the difference $\sigma_{\text{meas}}^2 - \sigma_{\text{in}}^2$ corresponds to the band broadening due to the HRP detector because variances are additive. The estimated value was found to be approximately $500 \mu\text{l}^2 \pm 100 \mu\text{l}^2$ which corresponds to a band volume of $20 \mu\text{l} \pm 10 \mu\text{l}$ for the HRP detector. It is important to note that, although the moving filter paper strip induced a $100 \pm$ seconds delay for drying and moving the observation vial, it did not produce extensive band broadening. Since the vial's flame and the solvent of the heavy area solution were supported by infrared lamps, the solvent were stopped into the minimum films of the paper which maintained their activities. By reducing the RF-HRP measuring tubing (34 μl) and using a microcatheter, it should be possible to minimize the band broadening even more.

Table 4.1 Wavelength Settings Employed and Chromatographic Parameters Observed by High Performance Liquid Chromatography with UV Absorption and Solid Solvents Room Temperature Fluorescence Spectroscopy Detection

Substrate	λ_{exc}^a nm	λ_{em}^b nm	V_{inj}^c nL	α^d	Efficiency ^e %	RT minutes
Salicylic	286(284)	335(325)	1.00	1.00	400	370
Phenanthrene	286(281)	436(425)	2.00	1.73	1000	1300
Pyrene	344(341)	373(375)	3.10	3.10	1000	900
Hexafluorene	363(353)	389(385)	4.36	3.65	1000	1000
Fluoranthene	363(360)	393(385)	5.10	3.00	1000	1000

^a The values in parentheses correspond to the wavelength UV emission values. The values are the selected wavelengths for the 10000 circumplexes

^b Emission values (λ_{em}) observed with a flow rate of 0.40 mL/min

^c Injection Volume (nL) calculated for a peak volume (V_{inj}) of 0.17 nL

^d Efficiency calculated using $2\pi(V_{inj}/V_{col})^2$ in which V_{col} is the peak width at 50% of the peak height expressed in volume units. Accuracy 1%

Flow rate effect. When a constant rate flows into the still flow zone and the strip starts moving, speed was maintained, we observed large variations of UV peak areas with the flow rate for fixed sample weight. Important variations of IRMP peak areas were observed with flow rate changes. The phosphorescent intensity was very dependent on the flow rate of the mobile phase. Figures 4-1 show the chromatographic IRMP response (IRMP peak area) versus flow rate. It can be seen that there is an optimum flow rate for maximum IRP signal and therefore for highest sensitivity. Several parameters related to the flow rate variation could be responsible for the observed phenomena. By keeping constant the filter paper speed, the amount of sample deposited per surface area of substrate increased with the flow rate. If a peak has a base width of one cm, the corresponding paper length on which the analyte would be spread is 11 cm. If the peak has a base width of 10 s, the same amount of sample would be spread on 1.1 cm and so on. Since the analyte was deposited on a shorter length of substrate, it would be reasonable to expect higher phosphorescent signals at high flow rates. However, by increasing the flow rate of the mobile phase, a longer column of solvent per substrate length was also delivered. Since the drying paper speed was kept constant, the drying time remained the same and might be insufficient for complete drying of the solvent. If this was the case, solvents could be responsible, in some extent, for quenching the phosphorescence signal. In addition, the increase in the flow rate was followed by an increase in the width of the sprayed area. Since the evaporation rate of the spray/distribution was kept constant, a possible diffusion of the analyte to the edges of the filter paper could also be responsible for the decrease observed in the phosphorescence intensities. With the exception of pyrene, all the other compounds showed the strongest phosphorescence signals between 1.1 to 2.0 ml/min and 2.0 to 3.0 ml/min. Considering the advantages of short samples like 1 ml of sample was chosen as the optimum mobile phase flow rate: resulting in a small analysis time of approximately 10 min per IRMP chromatogram.

Conclusion. Figure of Merit (FOM). Table 4-4 compares the AFM obtained with the UV absorption and the EPRF system for EPR detection. It is important to mention that both detectors were compared under experimental conditions for maximum EPRF sensitivity and reproducibility. The EPRF system was not optimized for UV absorption detection. The limits of detection and the reproducibilities of measurements obtained with the UV frequency source were comparable with those normally observed when these kinds of detectors are used for EPR analysis. When compared by EPRF, rhenium and phosphorescence showed calibration curves with larger linear dynamic ranges. Pyrene, detected strongly in the UV and as had a low limit of detection with the UV detector, the EPRF calibration curve for pyrene had a shorter linear dynamic range. In all cases, slopes close to unity and satisfactory correlation coefficients were obtained with both systems. The limits of detection with the UV detector were calculated from the equation $\lambda_{\text{LOD}} = 3\sigma_{\text{bkg}}/m$ where λ_{bkg} is the peak to peak background noise and m is the slope of the calibration curve [47]. The EPRF values were obtained by multiplying the equation above by the factor k_1/k_2 where k_1 is the integrated area in the sample compartment and k_2 is the total area of calibration on which the analysis had been applied. With both detector systems, rhenium, phosphorescence, and EPRF showed comparable limits of detection (LOD) in the nanogram range. The highest LOD value obtained for pyrene with the EPRF detector can be attributed to the weak phosphorescence signal presented for this phosphor under the experimental conditions employed in the study. The relative standard deviation obtained with the EPRF detector was within the reproducibility range of the technique (4% LOD), and no reported, was poorer than those obtained by UV absorption detection (15-2.6%).

Special Features. Although conventional UV absorption detectors operated at fixed wavelengths are able to discriminate between absorbing and non-absorbing species, they lack versatility and selectivity for the determination of absorbing compounds. The separation process in the chromatographic column has to be either complete or performed in such a

Figure 4-2: Room temperature gas/liquid chromatographic peak area (I_p) variations of acetamide **4**, phenanthrene **5**, pyrene **6** and benzo[a]pyrene **7** with acetic phase flow rate. Mobile phase: acetic acid. Sample size: 100 μ g of phenanthrene, 100 μ g of acetamide, injected volume 10 μ l.

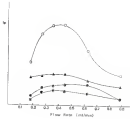


Table 4.4. Analytical Figures of Merit Obtained for High Performance Liquid Chromatography Using Solid Substrate Room Temperature Phosphorescence and UV Absorption Detection

Solute	LRP ^a	SRFP ^b	CORRELATION COEFFICIENT	LRP ^c (ng)
Acetaminide	3.0x10 ⁵ (3.0x10 ⁵)	1.0x10 ⁵ (10)	0.9910 (99)	0.770 (34)
Fluorenone	3.0x10 ⁵ (3.0x10 ⁵)	1.0x10 ⁵ (10)	0.9910 (99)	0.760 (34)
Pyrene	3.0x10 ⁵ (3.0x10 ⁵)	0.05x10 ⁵ (5)	0.9930 (99)	0.160 (63)
Benzo[<i>a</i>]pyrene	3.0x10 ⁵ (3.0x10 ⁵)	1.0x10 ⁵ (10)	0.9930 (99)	0.180 (63)

The values listed in parenthesis correspond to the AFM obtained with the UV detector

^a Linear dynamic range (LDR) was calculated by dividing the upper linear concentration by the limit of detection

^b Calculated from the curve log phosphorescence intensity (absorbance) versus log concentration

^c Signal-to-noise ratio = 3 and volume of 20 μ L (LRP) and 0 μ L (UV) were used to establish the limit of detection (LOD)

may also compound with signals overlapping near the detector. Thus again, this is a tedious procedure which usually involves either the optimization of a volume ratio between the solvent or the search for a consistent mobile phase. In addition, the detector wavelength does not usually coincide with the maximum absorbance peak of the desired compound which violates the sensitivity of HPLC.

Commercially available UV visible absorption detectors that consist of a scanning system or a photoconductor array with gaging system offer the possibility to select the best wavelength for each sample. If overlapped components reach the detector, the selection of an appropriate detection wavelength for a single compound is often difficult due to the usually broad absorbance bands.

Even though broad molecular phosphorescence bands commonly overlap, it is unusual for different compounds to have coincident spectra in such a way that neither excitation nor emission wavelengths can be selected to measure a single component of the mixture. This unique feature of HPLC is responsible for the high sensitivity of the technique [N₂, 10¹⁵-10¹⁶]. Figures 4 to 11 show the UV chromatogram of a mixture consisting of fluoranthene and pyrene along with the respective HPLC chromatogram. The chromatographic parameters of fluoranthene are listed in Table 4-3. From the UV chromatogram (Figure 4-4) it can be seen that complete resolution was not achieved by using pure methanol as the mobile phase. Although the UV absorption detection of other compounds is possible in these experimental conditions, the sample is useful to illustrate the selectivity of the HPLC detector. By mixing an HPLC and registering the phosphorescence emission at 441 nm, the HPLC chromatogram showed the presence of both solutes (Figure 4-5). When the detection wavelength was shifted to the maximum excitation and emission of fluoranthene, the phosphorescence of pyrene was no longer registered (Figure 4-6) and the single detection of fluoranthene was possible without the presence of pyrene in the chromatogram. Further identification of fluoranthene was then performed by stopping the HPLC paper strip at the position

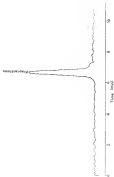
Figure 4.14 UV absorption chromatogram of a mixture containing 500 pg of chloramphenicol and pyrene. Mobile phase: acetonitrile. Flow rate: 2 ml/min; sample volume: 20 μ l.



Figure 4-6: (left) redoxstate (rhe temperature) dependence of a stress state (rhe) in a
 Thermodynamic and system (rhe) under (rhe) experimental conditions of Figure 4-6.
 (right) redoxstate (rhe) dependence of a stress state (rhe) in a



Figure 5 is a total substrate ions required phosphorylation diagram of a mixture containing 200 mg of phospholipase and 100 mg of substrate under identical experimental conditions of Figure 4. It is presented separately July 2000 in



phosphorescent intensity of the first eluted compound and comparing its emission spectrum with the corresponding spectrum of fluoranthene (see Figure 4-7). The spectral identification of pyrene was done in a similar way. The sharpness was stopped at the maximum phosphorescence intensity of the second eluted compound and the emission spectrum was registered at the maximum emission wavelength of pyrene. A spectrum with the same characteristics of the emission spectrum of pure pyrene was obtained (Figure 4-8). Spectral identification was also possible when both compounds were present at the same level of concentration in the substrate. By stopping the eluent prior only at the maximum phosphorescence intensity detected between the elution of the compounds, and irradiating the substrate at the maximum emission wavelength of pyrene, the presence of both analytes was confirmed by registering two phosphorescence bands with maxima around at 340 nm (fluoranthene) and 370 nm (pyrene) (see Figure 4-9). When the substrate was irradiated at the maximum emission wavelength of fluoranthene, the phosphorescence emission of pyrene was no longer detected (Figure 4-10). By comparing Figures 13 and 14, it can be noticed that even a weak phosphor like pyrene could be spectrally identified in the presence of a strong phosphor such as fluoranthene.

Conclusions

In this study, the feasibility of using HETP as a detection technique for GPC has been demonstrated. By using the new substrate assembly system, it was possible to perform GPC analysis in a continuous mode. The proposed detector has been evaluated by comparing its performance to a classical UV absorption detector under the same experimental conditions. A 14% efficiency loss was observed in the HETP chromatograms solely due to the UV absorption (HETP detector measuring using (1) µL) substrate and using filter paper strip. By reducing the length of the measuring tubing and using a mirror-substrate, it should be possible to eliminate the observed band broadening. Comparable RSD was obtained for both detection modes. By reducing the apparatus

Figure 4-7 (a) Room temperature phosphorescence emission (I_{p}) spectrum of the dioxo *o*-quinod compound using the excitation emission wavelength of Fluorescence (340 nm). (b) Room temperature phosphorescence emission spectrum of Fluorescence standard under the same experimental conditions of (a).

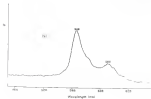
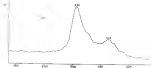


Figure 4-3 (a) Room temperature phosphorescence emission (λ_{em}) of the nitro-doped crystal registered in the vacuum condition overlength of pyrene (343 nm) (b) Room temperature phosphorescence emission spectrum of pyrene obtained under the same experimental conditions of (a)

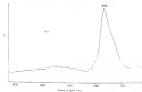


Figure 4: Time dependent fluorescence intensity (I_{F}) spectra of the solutions registered at the studied temperatures. Intensity derived between the duration of the two segments (indicated with arrows) is 100 ns.

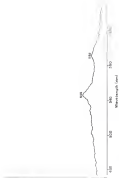
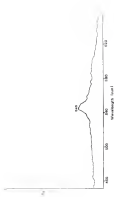


Figure 1.1: A graph showing the relationship between the length of a wire and its resistance.

Figure 4.10

Iron impurities phosphorescence emission (λ_{em}) spectra of the solutions registered at the maximum phosphorescence intensity showed increases the effect of the two compounds formation wavelength. (a) 10



collective and selective wavelengths of measurement, it was possible to characterize a single component of a mixture partially resolved by HPLC. This special feature makes the HPLC detector a useful tool for liquid chromatographic operations. Complex systems can be separated into simpler ones and the individual components of a mixture can be selectively determined by choosing the appropriate set of measurement wavelengths. The versatility of the new detector permits identification of compounds either from the retention time or from their HPL spectral characteristics, allowing the possibility for qualitative purposes. The greatest versatility, however, would result with the use of an identified photodiode array detector. This instrument would allow phosphorescence spectra to be recorded as the peaks elute producing "finger" prints to be resolved into individual components. We also believe that the HPLC detector could be very useful in cases such as forensic science where a permanent record of the analyzed samples would be extremely helpful. Compounds subjected to solid substrates and stored under a nitrogen atmosphere for several weeks have presented constant phosphorescence intensity (10-11). This offers the possibility of identifying the constituents of a stored sample at any required time. By knowing the position of every component on the HPLC paper strip, a new chromatogram (phosphorescence versus elution) can be obtained. If further identification is necessary, the unknown can then be mapped at the maximum phosphorescence intensity of every component to run its excitation and emission spectra. ADDITIONAL work, however, is necessary to determine the timing conditions for components of forensic interest.

CHAPTER 5

WADA GUIDELINES CONCERNING PROHIBITED SUBSTANCES OF DOPING, IDENTIFICATION AND TREATMENT IN SOME PERFORMANCE LEGAL CONSEQUENCES

Introduction

Informed by widespread cases of drug abuse by Olympic athletes to improve their physical performance under contest conditions, the International Olympic Committee (IOC) established a Medical Commission (MC) and charged it with the responsibility of controlling the abuse of performance-enhancing drugs (34,35). The MC developed a list of banned substances which includes over 100 different drugs and metabolites such as psychomotor stimulants, sympathomimetic amines, central nervous system stimulants, anabolic androgenic and anabolic steroids (36). Almost all banned drugs and metabolites are screened in urine, involving the screening analysis of a large number of urine specimens. Depending on the type of compounds, gas chromatography (GC), gas chromatography/mass spectrometry (GC/MS), high performance liquid chromatography (HPLC) and radioimmunoassay methods are usually employed for initial screening of urine samples (36). In all cases, the finding of a drug or metabolite by a screening procedure must be confirmed by a different analytical method of measurement.

Caffeine (1,3,7-trimethylxanthine) is a nervous system stimulant classified as a banned substance by the MC. Since it is considered to be part of the natural diet in man, a concentration limit of 12 µg/mL is allowed. Concentrations in urine above this limit are considered illicit. The abuse of caffeine by an athlete is usually indicated by MC screening tests. Its confirmation is then performed by HPLC or ultraviolet detection.

In this study, we are proposing the use of HPLC-MS/MS as an alternative method for the analysis of caffeine and its use

chlorophyllides (200) and chlorins, chlorophylls (2,3-200) and chloranthes (3,7-200) [21,22]. The APDS recorded with the HPLC detector are compared to those obtained by UV absorption detection under the same experimental conditions. The HPLC and UV chromatograms of spiked urine samples are compared, and the feasibility of coupling the HPLC chromatogram as a permanent record of the analyzed sample is discussed.

Instrumental

Instrumentation

The instrumental configuration employed in this study has been described in detail in Chapter 4. All the HPLC measurements were performed under a flow of dry nitrogen with a delay time of 0.53 s and a gate time for collection of data of 0.5 s. The excitation and emission filters were set to 25 nm and 5 nm, respectively. When needed a Perkin Elmer phosphorescence standard (200 nm/V) was employed for verification of possible intensity variations of the excitation source. The excitation and emission spectra were scanned at 120 nm/min rate and controlled by a Perkin-Elmer 8000 application program.

Reagents

"Reagent" pharmaceutical urine (Chemical Supply Corp.) and analytical reagent grade chemicals were used throughout. HPLC grade methanol was from Fisher Scientific Co. Caffeine, chlorophyllins and chloranthes were purchased from Sigma Chemical Co. and used without further purification. Permethrin sulfate (20) was obtained from Fisher Scientific Co., theanine (2) and urea (100a) was from Aldrich Chemical Co. and lead (II) acetate (100a) from Allied Chemical. Anhydrous ethanol (Fisher Scientific Co.) was used to prepare the heavy metal solutions. Polyphosphoric acid, Chemical Reagents Co. was employed as a drying substance to avoid the presence of humidity in a desiccator. 0.4 x 8 1000 a filter paper (Whatman and Whatman) was obtained as a 1.5 cm wide x 25 cm long filter paper roll and employed as a substrate. An activated glassfiber filter (Whatman Reagents) using 0.45 μ m pore size membrane was utilized as filter urine sample.

Procedure

The analysis solutions employed in this study were prepared in sequence using by serial dilution of stock solutions containing 100 µg/ml of active component and 1% v/v methanol as aid solubilization. A mixture of ethanol/water 40:60 v/v was used as solvent (1:1 H₂O, 0.1:0.9 Toluene, and 0.1:0.9 Toluene solutions). Fresh urine samples, obtained from volunteers not taking any medications were spiked with known amounts of the drugs. Before injection into the separation column, the spiked urine samples were filtered through an Acetate disposable filter assembly. After approximately 10 urine sample injections, partial stopping of the chromatographic column was observed as reflected by changes in retention times of the drugs. The heavy urine solutions were continuously sprayed onto the moving filter paper as a flow rate adjusted to deliver approximately 4 µl of solution per cm² of column area.

All the HRF measurements were performed by a procedure previously described in Chapter 4. A coupling time of 100 s and a scan interval of 0.2 s were employed to obtain 4000 points per HRF chromatogram. All HRF retention times were corrected with respect to delay times introduced by filter paper speeds.

Results and Discussion

As a first step toward obtaining a suitable heavy-ion reagent for the HRF analysis of caffeine, theophylline and theobromine, a study of their HRF characteristics was performed in the presence of three common heavy-ion salts, which included 1:1 H₂O, 0.1:0.9 Toluene, and 0.1:0.9 Toluene. The results are presented in Table 1-1. In agreement to results previously reported [4, 41-45, 64], all phosphates exhibit the highest HRF sensitivity in the presence of isopropanol. All compounds exhibited very similar phosphorescence excitation and emission wavelengths for each heavy-ion reagent. Because of the broad nature of HRF bands, the individual HRF detection of these phosphors in a mixture requires some kind of precise separation.

Caffeine-Ionic Effect. The phosphorescence intensity of caffeine, theophylline, and theobromine presented significant variations with the

Table 3-1
Room Temperature Phosphorescence Characterization of
Caffeine, Theophylline and Theobromine on Filter Paper/
Excerpt, Navy Atom Effect

Analyte ^a	Heavy Atom	λ_{ex} nm	λ_{em} nm	$I_1^{b,c}$	$I_1^{b,d}$	$I_{tot}^{b,e}$
Caffeine	T ^a	333	431	354	45	341
	Ti ^a	333	388	358	146	41
	Sn ^a	333	381	348	150	48
Theophylline	T	333	448	389	80	89
	Ti ^a	363	500	371	211	88
	Sn ^a	336	508	373	233	48
Theobromine	T	338	430	330	44	184
	Ti ^a	383	511	330	180	18
	Sn ^a	383	505	333	204	18

^a Concentrations used [8 pp-v] ¹

^b Average of three replicates

^c I_1 means phosphorescence intensity of the analyte plus heavy atom
(arbitrary units)

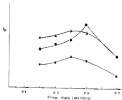
^d I_1 means phosphorescence intensity of the heavy atom blank
(arbitrary units)

^e I_{tot} means net phosphorescence intensity, $I \pm I_1 - I_1$

flow rate of the mobile phase. The possible reasons for this phenomenon were discussed in Chapter 4, when elution variations were observed in the HPL-EDRF analysis of several polynuclear aromatic compounds. Figure 3-1 shows the EDRF response of acridine, naphthylamine, and thianthrene relative to the flow rates studied. The highest ERF signals were obtained between 0.4 and 1.1 mL/min. Considering the reduction in the ERF signal response of thianthrene (approximately 50%) when the flow rate was varied from 0.2 to 0.4 mL/min, and the advantage of thianthrene analysis due to about 0.2 mL/min at the flow rate to perform the separation with this flow rate, a separation time of 4 minutes per sample was achieved. The total analysis time, however, depended on the speed of the moving paper strip. As indicated in Chapter 4, the transport of the eluted compounds from the exit of the microtiter to the sample compartment of the spectrophotofluorometer induced a delay time. By increasing the filter paper speed, this delay time can be reduced resulting in a shorter analysis time.

Filter Paper Speed, EDRF. In order to obtain the thianthrene profile analysis time with the maximum EDRF detector, we altered the ERF measurement at the fastest filter paper speed supported by the autosampler controller filter (20 mL/min). Unfortunately, at this substrate speed we were not able to detect ERF analysis from any of the studied compounds. For a constant spraying flow rate, the amount of analyte deposited per cm^2 of filter paper only depends on the substrate speed. At the fastest filter paper speed, the analysis deposition is performed over the longest number of substrates, resulting in the smallest amount of analyte deposited per cm^2 of filter paper. In addition, at 20 mL/min filter paper speed the drying time is the shortest, and a frequent strip needs approximately 1 min. in the drying chamber. Considering the loss of ERF signals to the insufficient amount of analyte sprayed per cm^2 of filter paper and possible substrate quenching due to short drying time, we reduced the speed of the filter paper strip. Several substrate speeds ranging from 1.5 to 16 mL/min, were tested for highest ERF association. Figure 3-2 shows the EDRF chromatograms obtained at these different

Figure 3-1. Solid substrate room temperature phosphorescence peak area (I_{sp}) variations of theobromine \bullet , theophylline \blacktriangle and caffeine Δ with mobile phase flow rate variations. Mobile phase: methanol/water 11/45 v/v. Sample size: 400 μ g of each compound. Injected volume: 20 μ L.



paper speeds, of a synthetic station containing thiophylline, theophylline, and caffeine. The mobile phase employed for separation was a 10:10:90 methanol/water solution. At a filter paper speed of 18 cm/min (Figure 3-3a), a partially unsaturated sample was still presented to the HPLC detector. In addition, not enough analyte per cm^2 of substrate was properly exposed to produce acceptable HPL signal intensities. Higher HPL signal intensities were observed at 5.5 cm/min filter paper speed (Figure 3-3b), when the analyte coated approximately 4 min and 40 s in the drying phase. However, at such a low filter paper speed, the analyte diffusion on the substrate increased due to the high volume of mobile phase applied in a short section of filter paper strip. As a consequence, broadened and asymmetric peaks were observed resulting in a decrease in the chromatographic efficiency. As a compromise between sensitivity and peak profiling, a paper speed of 11.1 cm/min gave the best results for HPLC detection (Figure 3-3c). By employing this substrate speed, a delay time of approximately 7 min and 13 s was observed in the HPLC chromatogram. The total HPLC/HPLC analysis time was about 13 min and 17 s per sample. All the HPLC chromatograms presented in this chapter have been referenced for the delay time (7 min and 13 s). It is important to point out, however, that the optimum substrate speed for maximum HPL sensitivity and chromatographic efficiency depends on the flow rate and the nature of the mobile phase. The use of a more volatile mobile phase would require shorter drying times, resulting in faster paper speeds. In this case, though, the limiting factor of substrate speed rests probably in the amount of analyte exposed per cm^2 of filter paper. This amount could be easily increased by striking at higher flow rates, which would result in the advantage of shorter analysis times.

Chromatographic Peak Broadening. The peak efficiencies were obtained according to Gaussian peaks and are listed in Table 3-2. As observed, there was a considerable loss of efficiency (approximately 77%) when the HPLC chromatograms were compared to those obtained by GC detection. This efficiency loss is approximately 3 times higher than the one observed in the comparative analysis of several polycyclic aromatic compounds by HPLC

Figure 5.5: Solid sublimates and nonaqueous azeotropic vapours (1_g) of chloroform (11), chlorophyllin (11) and caffeine (13) versus 2110Å paper speed. $\omega = 1.6$ cm/min, $\delta = 3.5$ cm/min, $\phi = 11.5$ cm/min.

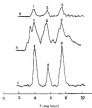


Table 3.3: Chromatographic Parameters Obtained by UV Absorption and HPLC Detection in the HPLC analysis of Theobromine, Theophylline, and Caffeine

Solutes	V_R^a min	k' ^b	Efficiency ^c	
			UV plates	HPL plates
Theobromine	1.48	8.47	6156	187
Theophylline	1.48	4.37	3968	94
Caffeine	1.48	2.15	349	57

^aRetention volume (V_R) obtained with a flow rate of 0.5 mL/min

^bCapacity factor (k') calculated for a dead volume of 1.17 mL

^cEfficiency calculated using $N = 5.54 (V_R/V_{0.5})^2$ in which $V_{0.5}$ is the peak width at 50% of the peak height expressed in volume units. Accuracy 10%

with HPLC and UV detection (see Chapter 4). In that case, pore method was employed as a mobile phase. The chromatographic separation of caffeine, theophylline and theobromine required the use of a mobile phase composed by methanol-water 20:80 v/v. This solvent has a poorer volatility than acetonitrile and requires longer drying times. As mentioned earlier, the presence of solvent in the substrate increases the diffusion of analytes and favors its band broadening and loss of chromatographic efficiency. In future applications of the HPLC detector for HPLC analysis, it would be convenient to choose the solvent based not only on its ability to separate the analytes of interest but also on its volatility.

Initial Fluxes of PAHs, APOH Table 1-3 compares the APOH obtained with the UV absorption and the HPLC system for HPLC detection. Both detectors were compared under experimental conditions for various HPLC sensitivity and reproducibility. The limits of detection with the UV detector were calculated from the equation $S_L = 3\sigma / (1/\alpha) \cdot 10^3$ where $1/\alpha$ is the peak-to-peak background value and σ is the slope of the calibration curve [42]. The HPLC values were estimated by multiplying the equation above by the factor A_s/A_t , where A_s is the background area in the sample component and A_t is the total area of substance on which the analysis has been applied. The LOD of all studied compounds was in the nanogram level for both detectors. The HPLC values were comparable with data previously reported in studies involving the optimization of parameters for HPLC detection [43,44]. The same trend was observed for the UV LOD, which were in the same level of those obtained in the analysis of urine samples by HPLC-UV absorption detection [45-47]. The LOD achieved by HPLC are approximately one order of magnitude larger than those obtained by UV absorption. This is in agreement with the LOD estimated, since the HPLC values are from about 1 to 5 times lower than the UV ones. It is important to mention, though, that no efforts were made in order to obtain the upper limit of linear concentration of polycyclic aromatic. The relative standard deviations (based on triplicate measurements) of the UV absorption detection ranged from 16 (at medium concentrations) to 18 (at low (1-16 ppm) and high (100-300 ppm) concentrations). As reported the

Table 5.1 Analytical Figures of Merit Obtained for Theocofline, Theophylline and Caffeine by High Performance Liquid Chromatography with Solid Substrate Benz Triphenylmethyl Fluorophenyl and 20 Detection

Substrate	LSR ^a	Slope ^b	Correlation Coefficient	LSR ^c (ng)
Theocofline	1.5x10 ³ (1.5x10 ³)	8.8178 (8)	0.9982 (998)	1.5 (1.5)
Theophylline	1.5x10 ³ (1.5x10 ³)	8.8178 (8)	0.9982 (998)	1.5 (1.5)
Caffeine	5.5x10 ³ (5.5x10 ³)	8.8178 (8)	0.9982 (998)	1.5 (1.5)

All LSR were obtained using experimental conditions for maximum S/N ratio sensitivity and reproducibility. The values listed in parentheses correspond to the LSR obtained with the UV detector.

^aLinear dynamic range (LDR) was calculated by dividing the upper linear concentration by the limit of detection.

^bCalculated from the curve log phosphorescence intensity (absorbance) versus log concentration.

^cTypical detection limits = 1 and volume of 10 µl (HPLC) and 1 µl (UV) were used to calculate the limit of detection (LOD).

HEPT measurements presented higher AED values than the TF ones and depended on the studied compound. For illustration, the AED ranged from 84 (low concentrations) to 116 (high concentrations) with no improvement in urine concentrations (64) caffeine and theophylline showed an of 7.5 and 6% at low, medium and high concentrations, respectively.

HEPT Detection of Caffeine, Theophylline, and Theobromine in Urine Samples

Peak urine samples were spiked with known amounts of caffeine, theophylline and caffeine. After filtration, the samples were injected in the chromatographic system. Under the optimized conditions employed, blank urine presents peaks in the TF chromatogram (see Figure 3-1). Although theophylline and caffeine are well resolved, theobromine appears however as urine peaks seriously compromising the determinability of this compound. In the other hand, the HEPT detector produces a clear chromatogram free from blank urine interference. This is due to the essentially non phosphorescent nature of proteins in room temperature [81-83]. Previous studies involving the HEPT determination of PAHs in urine samples without previous separation [84-85] have shown that the matrix noise responsible for the most phosphorescent nature of urine do not have significant contribution to the background signal of solid substrates. Thus the magnitude of the HEPT signals of the three drugs in spiked urine samples and aqueous solutions are within the standard deviations of measurements, and the blank response is smaller in both cases. We believe that HPLC-HEPT could be employed as an alternative method for the analysis of urine samples.

As mentioned in Chapter 4, the use of HEPT detection offers the possibility of identifying the constituents of a tested sample at any required time. This is an additive benefit for urine which a permanent trend of the analyzed sample is of interest. As a concrete means of evaluating this possibility for the specific case of caffeine, theophylline and theobromine, the first peak HEPT corresponding to a chromatogram of a mixture of the three compounds was tested in a detector at room temperature treated with absolute EtOH and in the

Figure 4. Isoprenoid levels in the *Microcystis* strains by day in the laboratory. The data were analyzed by ANOVA. The error bars represent the standard deviation. The number of replicates was 30.



presence of anhydrous CaCl_2 . The relative positions of the stained phosphors on the filter paper strip were measured and marked with a pencil on the edge of the substrate. A new "autoradiogram" of anhydrous RFP intensity versus distance was then obtained. One month later the filter paper strip was removed from the darkroom and placed on the filter paper front of the microfilm system for RFP identification and quantitation. The detection parameters were the same as those utilized in the measurements of the fresh sample. As expected, the relative position of the stained compounds on the substrate strip remained constant, allowing RFP identification based on their phosphorescence signal versus distance. Searching for further identification, the filter paper strip was stripped at the maximum RFP signal intensity of each compound and the phosphorescence spectra were recorded. The excitation and emission spectra of these phosphors obtained with the fresh sample and one month later are shown in Figures 3-4, 3-5, and 3-6. Figure 3-7 shows the spectra of the blank obtained under the same experimental conditions, after one month of storage time. Significant RFP intensity reductions and changes in maximum wavelengths were observed in all analysis spectra. The background spectrum, though, remained approximately the same. Table 3-8 summarizes the modifications observed. There is a small shift to the blue ($\sim 5 \text{ nm}$) in the excitation spectra of all phosphors. The relative ratios were displaced to a region of longer wavelengths and varied with the stained compounds. Possible variations in the intensity of the excitation ratios were investigated by comparing the RFP signal intensities of a phosphorescence standard (100 ng/100 nm) obtained at the moment of detection of fresh and one month old samples. No significant variations were observed, illustrating the accuracy of signal normalization. However, RFP intensity reductions of about 2.5, 2.8, and 2.9 times were verified for theobromine, theophylline and caffeine respectively. Since a significant decrease in the background signal was not observed, there was a reduction in the signal to background ratio of all phosphors. These modifications obviously make difficult the identification and quantitation of the stained compounds. It is important to notice, though,

Figure 5-5 Room temperature phosphorescence excitation (blue) and emission (red) spectra of the reaction in 501 (blue) and 502 (red) samples applied with samples sprayed on filter paper. (a) after one week storage of filter paper substrate

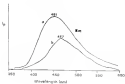


Figure S 3 Room temperature phosphorescence excitation (Em) and emission (Ex) spectra of theophylline in (a) fresh baked crumpled paper spread on silica paper, (b) dried the north storage of silica paper substrate

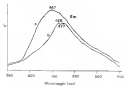


Figure 3-4 Base composition (phosphate and nucleoside) and nucleoside (base) species of nucleoside in (a) fresh spiked urine samples exposed on filter paper, (b) after one month storage of filter paper substrate

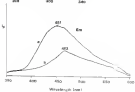


Figure 3.3 Room temperature phosphorescence excitation (blue) and emission (red) spectra of various samples sprayed on E1000 paper in the presence of LB 01.

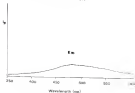


Table 3.4. Effect of Mixture Size, the Room Temperature Fluorescence Characterization of the Aromatic Phosphorites, and Catalysts

Compound	Probe Temp ^a		Room Temp. Laser			
	J_{th} (m)	J_{th} (cm)	I_{th}	I_{th}^{b} (cm)	I_{th}	I_{th}^{b}
Phosphorite	175	5.5	117	2.8	271	445
Phosphorite	175	5.5	14	2.8	275	555
Catalysis	175	5.5	170	5.8	275	445
Blank						

^aTemperature 20 °C.

^bFluorescence intensity (arbitrary unit); obtained by I_{th} or I_{th} . I_{th} stands for the average level of the signal + blank and I_{th} is the blank signal. I_{th} and I_{th} were obtained at wavelengths 445 nm and 555 nm.

Intensity provided by each analysis in the blank sample. Signal in background (m) is 0.01 mW and dividing I_{th} by I_{th} .

that no attempts were made to optimize the storage conditions. The presence of moisture in the desiccator could be an even more serious responsible for the variations observed in the HPT signals. Storage of the filter paper strips under a dry atmosphere of an inert gas would minimize moisture effects. The shifts observed in the various analyses involving the suggest that sample degradation occurred on the filter paper strip. This possibility stresses, one more time, the necessity of a careful study involving the search for optimum storage conditions. Keeping the filter paper strip at low temperature could minimize degradation of the samples.

Conclusions

In this chapter, we have demonstrated the possibility of using HPLC-HPT as an alternative method for the quantitative analysis of caffeine, theobromine and theophylline in urine samples. After responsible to them designed by UV absorption detection was achieved by HPT analysis. The experimental conditions employed produced UV chromatograms with urine peaks that seriously compromise the discrimination of theobromine. The non-phosphorescent nature of urine, however, allows the HPT detection of theophylline free from blank interferences.

The feasibility of using HPT chromatograms as permanent records of analyzed samples strongly depends on the search of appropriate storage conditions. In the specific case of caffeine, theobromine and theophylline, the storage of filter paper strips in a desiccator at low temperature was not effective enough to avoid degradation of the compounds. This fact, however, does not exclude the possibility of employing HPLC-HPT as a confirmation method for caffeine done by urine. The LRI obtained by HPT allows the detection of lower concentrations of caffeine than the upper limit established by the GC (12 µg/mL). Since a small number of urine samples per sports event usually requires the verification of positive screening tests, the longer this necessary for HPT analysis does not represent a serious disadvantage when the method is required in UV absorption detection.

CHAPTER 8

CONCLUSIONS AND SUGGESTIONS FOR FUTURE WORK

During the last two decades, RHP has been considered among the phosphorimetry techniques as the most suitable approach to be applied in routine analysis of a large number of samples. The simplicity of the sampling procedure, eliminating the need for expensive equipment and for transportation of samples, and the possibility of automation have been pointed out as the main advantages forward over LP, DRHP and RPL. In applications areas where the samples are small and precious, such as clinical chemistry, toxicology and nutrition, the small sample requirement of RHP associated to its high sensitivity and selectivity are equally important.

Although it is the simplest phosphorimetry technique to work with, its application to routine analysis of a large number of samples has been limited by the manual procedure commonly employed in RHP analysis. Sample preparation (previous several manual steps which can lead to appreciable random errors) requires some degree of experimentation, experience, and consumes between 4 to 12 minutes per sample. The new automatic system developed in these studies has eliminated the manual steps and allows performance of 64 and 96 measurements per sample. By using appropriate solubilizers, small volumes of samples are conveniently sprayed on filter paper substrates ($\sim 3 \mu\text{l}/\text{cm}^2$) producing the illumination in areas where the availability of samples is limited. The possibility of testing many new mixtures in their optimum concentration range, and the achievement of ARL comparable to those obtained by manual RHP procedures suggest that the proposed system is a convenient approach to develop the full potential of the technique as an automated tool for routine analysis.

The versatility of the ion selective automatic system allows us perform HPLC analysis in a continuous mode. This is an attractive feature for its application in flowing systems. By employing FIA as a continuous sample introduction technique, calibration curves were easily obtained with only one or two each analyte solution. When combined with HPLC, the performance was comparable to HPLC chromatogram detection. The high selectivity of HPLC makes the proposed system a useful tool for liquid chromatographic separation. By choosing the appropriate set of measurement wavelengths, individual components of mixtures partially resolved by HPLC can be selectively determined. Identification of compounds other than the retention times or their HPLC spectral characteristics is possible, showing the potential of the HPLC detector for qualitative purposes. If needed, the selectivity can be improved by HPLC. By using the appropriate combination of heavy atom molecules and suitable wavelengths, it is possible to enhance the phosphorescence signal of a target compound in the presence of other phosphors. This resolved phosphorescence can also be used to improve the selectivity of the new system. Its application, however, is restricted by the stability of phosphorescence lifetimes at room temperature. Synchronous excitation phosphorescence should also be considered as a possibility of improving the selectivity of the HPLC system, but its employment requires the use of a detection unit different than the one utilized in these studies.

When compared to HPLC-MS/MS, HPLC-HPLC offers several advantages. It can be applied to a wider variety of phosphors, since some compounds form strong phosphorescence on solid substrates than in strongly solvated solutions. The collection of phosphorescence on solid substrates does not require desorption of complex which leads to a simpler procedure and shorter analysis time. Finally, the number of publications involving HPLC studies contains HPLC published here. This fact facilitates the optimization of parameters for a larger number of compounds when HPLC is applied as a HPLC detection technology.

The use of the HMTF detector for HPLC analysis is feasible in all cases where phosphorescent compounds need to be determined. Its utilization, however, is particularly interesting in those cases where a permanent record of the analyzed samples is of interest. The storage of samples sprayed on ELNES paper enables within the possibility of identifying the constituents of the samples at any required time. The relative position of the stored compounds on the substrate strip allows the identification based on phosphorescence signal versus distance. Further identification based on HPL spectral characterization, though, strongly depends on the choice of appropriate storage conditions. Future work needs to be done in this area, seeking optimum storage conditions for compounds of interest.

References

1. J.S. Winefordner, E.E. Schuman, and E.G. W'Hever, *Luminescence Spectrometry in Analytical Chemistry*, Wiley-Interscience, New York, 1971.
2. E.E. Schuman, *Molecular Luminescence Spectroscopy Methods and Applications Part I*, Wiley-Interscience, New York, 1970.
3. E.E. Schuman, *Molecular Luminescence Spectroscopy Methods and Applications Part II*, Wiley-Interscience, New York, 1971.
4. F. S. Dole, *Atom Fluorimetry: Fluorimetry for Chemical Analysis*, Wiley-Interscience, New York, 1966.
5. F.E. Schuchman and E. Lander, *Pure & Appl. Chem.*, 51, 1703 (1961).
6. E.E. Schuchman, *J. Chem. Educ.*, 44, 523 (1970).
7. R.P. Fether, R.E. Frieslander, and E.E. Schuman, *Anal. Chem.*, 40, 125, 2 (1968).
8. J.L. Goff, R.L. Wilton, and J.S. Winefordner, *Talanta*, 18, 351 (1971).
9. R.L. Wilton, *Anal. Chem.*, 36, 1748 (1964).
10. R.L. Wilton, *Anal. Chem.*, 36, 174 (1964).
11. R.P. Fether and J.S. Winefordner, *Anal. Chem.*, 44, 548 (1972).
12. R.P. Fether, R.E. Frieslander, E.E. Schuchman, and E.E. Schuman, *Anal. Chem.*, 51, 1821 (1971).
13. R.J. Salvo, R.E. Wilton, Jr., and R.E. Schuchman, *Anal. Chem.*, 39, 180 (1967).
14. G. Wilton and F.E. Wehrhald, *J. Phys. Chem.*, 61, 1076 (1957).
15. R.P. Wilton, *J. Inorg. and Nucl. Chem.*, 31, 475 (1963).
16. E. Schuchman, *J. Opt. Soc. Am.*, 58, 448 (1966).
17. E. Doolinger and J.S. Winefordner, *Anal. Chem.*, 42, 438 (1970).

14. R. J. Barabian, *Anal. Chem.* **55**, 449a (1983)
15. J. L. Ward, G. L. Wilson, and J. B. Winfallinger, *Science* **19**, 394 (1981)
16. E. R. Behrman and G. Walling, *Science*, **176**, 55 (1972)
17. E. R. Behrman and G. Walling, *J. Phys. Chem.* **77**, 582 (1973)
18. R. Amphlett-Baker, T. Ansel, and R. Vincent, *Chem. Phys. Lett.* **39**, 267 (1975)
19. R. Almgren, F. Grisser, and J. R. Thomas, *J. Am. Chem. Soc.* **101**, 179 (1979)
20. R. Almgren, F. Grisser, and J. R. Thomas, *J. Am. Chem. Soc.* **104**, 193 (1982)
21. L. J. Glass-Lew, R. Heiler, and J. R. Behrman, *Anal. Chem.* **51**, 79 (1979)
22. R. Barlier and L. J. Glass-Lew, *Anal. Chem.* **52**, 1559 (1980)
23. J. J. Zenderiktsch, J. J. Glass, G. Gerdjar, R. V. Frei, and R. R. Velthoven, *Science* **19**, 767 (1981)
24. J. J. Zenderiktsch, G. Gerdjar, R. R. Velthoven, and R. V. Frei, *Anal. Chem.* **54**, 814 (1982)
25. J. J. Zenderiktsch, R. J. A. van Hilsum, R. G. Gerdjar, R. R. Velthoven, and R. V. Frei, *Chromatographia* **13**, 347 (1981)
26. R. Eick, *J. Chromatogr.* **50**, 178 (1967)
27. R. A. Reynolds, J. L. Wilson, and J. B. Winfallinger, *Anal. Chem.* **48**, 716 (1976)
28. J. L. Wilson, R. A. Reynolds, and J. B. Winfallinger, *Spectrochim. Acta* **30A**, 2619 (1974)
29. E. R. Behrman and R. T. Parker, *J. Phys. Chem.* **81**, 1831 (1977)
30. R. J. A. van Nieuwenhise and R. J. Barabian, *Anal. Chem.* **49**, 1794 (1977)
31. R. J. A. van Nieuwenhise and R. J. Barabian, *Anal. Chem.* **49**, 1846 (1977)
32. R. E. Ford and R. J. Barabian, *Anal. Chem.* **50**, 626 (1978)
33. R. E. Ford and R. J. Barabian, *Anal. Chem.* **51**, 104 (1979)

- 38 R. E. Hesterman and R. J. Harrison, *Anal. Chem.* **34**, 2477 (1962).
- 39 R. J. Harrison and W. A. Smith, *Anal. Chem.* **32**, 1145 (1960).
- 40 R. A. Seltzer and R. J. Harrison, *Anal. Chem.* **34**, 1894 (1962).
- 41 R. A. Seltzer and R. J. Harrison, *Anal. Chem.* **36**, 226 (1964).
- 42 R. E. Parker, R. E. Fowell-Smith, and R. E. Peck, *Anal. Chem.* **33**, 128 (1961).
- 43 R. L. Holliman and R. E. Dorsey, *Anal. Chem.* **34**, 1944 (1962).
- 44 T. Ye. Blak and J. B. Winfordman, *Appl. Spectrosc. Rev.* **1**(2), 395 (1971).
- 45 T. Ye. Blak, G. L. Solov, and J. B. Winfordman, *Anal. Chem.* **45**, 1118 (1973).
- 46 E. Lee Yee Hwang and J. B. Winfordman, *Anal. Chem. Acta*, **304**, 1 (1975).
- 47 G. E. Ford and R. J. Harrison, *Anal. Chem.* **31**, 595 (1959).
- 48 G. J. Riley and F. G. Seybold, *Anal. Chem.* **38**, 1577 (1976).
- 49 W. L. Long and J. B. Winfordman, *Anal. Chem.* **34**, 154 (1962).
- 50 J. L. Ward, R. L. Newbauer, and J. B. Winfordman, *Talanta* **10**, 719 (1963).
- 51 R. F. Smith and J. B. Winfordman, *Talanta* **10**, 715 (1963).
- 52 E. T. Yu, R. L. Nelson, and J. B. Winfordman, *Chem. Phys. and Spectrosc. Instrumentation*, **13**(1), 95 (1961).
- 53 R. L. Holliman and R. E. Dorsey, *Anal. Chem.* **36**, 908 (1964).
- 54 R. D. Sharpfilla and G. E. Solov, *Anal. Chem.* **34**, 2012 (1962).
- 55 F. G. Seybold and R. Wilson, *Anal. Chem.* **47**, 1594 (1975).
- 56 T. Ye-Blak, E. Lee Yee, and J. B. Winfordman, *Anal. Chem.* **44**, 1168 (1972).
- 57 T. Ye-Blak, E. Lee Yee, and J. B. Winfordman, *Talanta* **16**, 548 (1977).
- 58 L. B. Jurekiewicz, *Anal. Chem.* **49**, 1888 (1977).
- 59 T. Ye-Blak and J. B. Winfordman, *Anal. Chem.* **51**, 971 (1979).

48. B. Lee Van Nostrand and J. D. Winefordner, *Anal. Chim. Acta* 104, 119 (1979).
49. R. F. Smith and J. D. Winefordner, *Anal. Chem.* 52B, 372 (1980).
50. R. F. Smith and J. D. Winefordner, *J. Pharm. Biomed. Anal.*, 1, 113 (1983).
51. R. F. Smith, R. S. Fynsboerger, J. B. Scholten, and R. B. Seeling, *Anal. Chem.*, 55, 1031 (1983).
52. J. J. Aaron, R. Smith, and J. D. Winefordner, *Anal. Chim. Acta* 148, 171 (1984).
53. J. J. Aaron, R. B. Scholten, and J. D. Winefordner, *J. Agric. Food Chem.*, 31, 1222 (1983).
54. J. J. Vanevski and R. B. Scholten, *Anal. Chem.* 56, 1958 (1984).
55. R. Y. Ho, K. Asakura-Ajiya, and S. Gosh, *Analytica* 109, 3519 (1984).
56. C. B. Salton, R. B. Scholten, and J. D. Winefordner, *Anal. Chem.* 58, 1187 (1986).
57. C. B. Salton, R. B. Scholten, K. Asakura-Ajiya, R. S. Fynsboerger, A. B. O'Reilly, T. B. Kinnear, and J. D. Winefordner, *Anal. Chim. Acta*, 45, 419 (1988).
58. R. B. Salton, K. Asakura-Ajiya, C. B. Salton, A. B. O'Reilly, and J. D. Winefordner, *Anal. Chim. Acta*, 204, 167 (1989).
59. L. B. Parry, A. B. Kneipflich, and J. D. Winefordner, *Anal. Chim. Acta*, 915, 223 (1991).
60. L. B. Parry, A. B. Kneipflich, and J. D. Winefordner, *Anal. Chem.*, 61, 2129 (1989).
61. B. L. Van Nostrand and J. D. Winefordner, *Appl. Spectroscopy* 32, 7 (1978).
62. R. B. Brown, *Introduction to Instrumental Analysis*, McGraw-Hill, New York, 1987.
63. R. B. Asakura-Ajiya, J. J. Van, and R. Y. Ho, *Anal. Chem.* 57, 829 (1985).
64. T. Van Nostrand and R. B. Scholten, *Anal. Chem.* 58, 1954 (1986).
65. C. B. Salton and R. B. Scholten, *Anal. Chem.* 59, 1678 (1987).
66. C. B. Salton and R. J. Portchell, *Anal. Chem.*, 61, 1463, 1465 (1989).
67. J. Barucha and R. B. Brown, *Prec. Inorganic Analysis, Chemical Analysis*, Vol. 4B, 2nd Edition Wiley, New York, 1988.

- 40 A. R. Barlett and D. A. Cowan, *Int. J. Spectrosc.* **17**, 185 (1978).
- 41 A. R. Barlett, *J. Amer. Sci.* **3** 183 (1985).
- 42 D. R. Collins, A. C. Kummer, C. E. Kotton, W. E. Schram, and J. L. Kordick, *Clin. Chem.* **33**(2), 348 (1987).
- 43 D. Kozubski, E. Ben-Del, E. Christakos, H. J. Arend, and L. Brown, *Prog. Steroid. Biogen.* **19**, 434 (1985).
- 44 F. L. H. Tan, C. E. Sallis, D. W. Baskin, E. J. Kelenoski, and E. Seylanian, *J. Pharm. Sci.* **70**, 395 (1981).
- 45 E. F. Borch and J. D. Winefordner, *Anal. Lett.* **11**(16), 173 (1962).
- 46 H. H. Ammon, D. B. Saline, and J. D. Winefordner, *Spectrochim. Acta*, **41A**, 417 (1985).
- 47 H. F. Borch and J. D. Ammon, *Anal. Chem.* **55**, 173 (1983).
- 48 L. R. Perry, E. Y. Hsu, and J. D. Winefordner, *Talanta*, **34**(5), 1437 (1989).
- 49 E. Kloman and E. Gurevitz, *J. Lig. Chem.* **4**(3), 495 (1960).
- 50 H. Y. H. Hsiao, S. Tsuruta, M. Iguchi, and H. R. Kaelin, *J. Lig. Chem.*, **7**(3), 1995 (1964).
- 51 C. F. Papadimitrakia and E. Gurevitz, *Kinetica J.* **28**, 181 (1967).
- 52 E. Saline, E. Himmert, C. Schuster, and E. Hsu, *J. Chem.* **4**(1), 173 (1987).
- 53 J. E. Nelson, in *Fluorimetric Analysis, Modern Methods*, Part 4, Chapter 5, Marcel Dekker, Inc. New York 1981.
- 54 H. F. Borch, D. B. Saline, and J. D. Winefordner, *Anal. Chem.* **49**, 146, 157 (1986).
- 55 H. F. Borch, E. F. Borch, J. D. Winefordner, and E. E. Nelson, *Clin. Chem.* **28**(7), 1261 (1984).

BIOGRAPHICAL SKETCH

Arduus Rebel Campiglia, son of Rebe Rebel Guillem and Delia Kelly B Campiglia de Rebel, was born February 24 1942, in Los Pinos, Uruguay. In 1974, he moved with his family to Brasília, Brazil, where he completed his high school studies. He entered University of Brasília, Brasília DF, in March 1979 and received the degree of Bachelor of Chemistry in November 1981. In March 1981, he entered graduate school in chemistry at University of Brasília. In 1984, he was hired by the Chemistry Department of that university as an assistant professor. The degree of Master of Chemistry was received from the University of Brasília in June, 1985, where he continued as an assistant professor until July 1986. After being awarded with a four year Fellowship from Coordenação de Aperfeiçoamento de Pessoal de Nível Superior (CNPq) to continue his studies in chemistry, he entered the graduate program in chemistry at the University of Florida in August 1986 and received the degree of Bachelor of Philosophy in June, 1988. Arduus B Campiglia is currently an assistant professor at the Chemistry Department of the University of Brasília.

I certify that I have read this study and that in my opinion it conforms to acceptable standards of scholarly presentation and is fully adequate in scope and quality as a dissertation for the degree of Doctor of Philosophy


James E. Strickland, Chairman
Graduate Research Professor
of Chemistry

I certify that I have read this study and that in my opinion it conforms to acceptable standards of scholarly presentation and is fully adequate in scope and quality as a dissertation for the degree of Doctor of Philosophy


Clifford S. Brown
Associate Professor of Chemistry

I certify that I have read this study and that in my opinion it conforms to acceptable standards of scholarly presentation and is fully adequate in scope and quality as a dissertation for the degree of Doctor of Philosophy


Vanessa L. Young
Associate Professor of Chemistry

I certify that I have read this study and that in my opinion it conforms to acceptable standards of scholarly presentation and is fully adequate in scope and quality as a dissertation for the degree of Doctor of Philosophy


Stephen D. Johnston
Professor of Chemistry

I certify that I have read this study and that in my opinion it conforms to acceptable standards of scholarly presentation and is fully adequate in scope and quality as a dissertation for the degree of Doctor of Philosophy



Eric Allen
Professor of Environmental
Engineering Science

This dissertation was submitted to the Graduate Faculty of the Department of Chemistry in the College of Liberal Arts and Sciences and to the Graduate School and was accepted as partial fulfillment of the requirements for the degree of Doctor of Philosophy

August 1998

DALE EMMETT HENRI